DESIGN AND ANALYSIS OF ELECTROHYDRAULIC SERVOVALVE

by

JAI NARAYAN

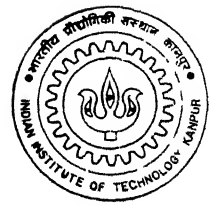

DEPARTMENT OF MECHANICAL ENGINEERING

INDIAN INSTITUTE OF TECHNOLOGY KANPUR

APRIL, 1997

DESIGN AND ANALYSIS
OF
ELECTROHYDRAULIC SERVO VALVE

A Thesis Submitted

in Partial Fulfillment of the Requirements
for the Degree of
MASTER OF TECHNOLOGY

by

Jai Narayan

To The
DEPARTMENT OF MECHANICAL ENGINEERING
INDIAN INSTITUTE OF TECHNOLOGY, KANPUR

1997

ME-1997-M-NAR-DES

CERTIFICATE

It is certified that the work contained in the thesis entitled " **Design and analysis of Electrohydraulic Servovalve"** by Jai Narayan has been carried out under my supervision and it has not been submitted elsewhere for a degree

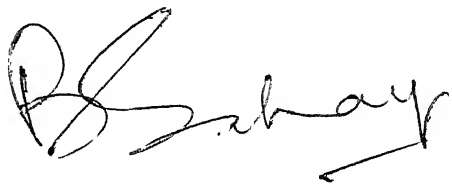

Dr. Birendra Sahay
Professor and Head of the Department
Department of mechanical engineering
I I T Kanpur

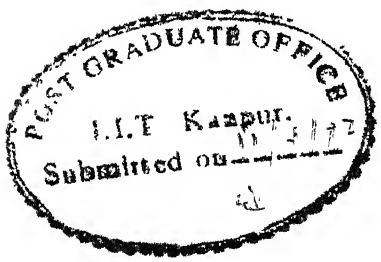

Acknowledgment

I take this opportunity to express my deep sense of appreciation and gratitude to my guide Prof. Birendra Sahay for offering me to work on electrohydraulic servovalve which will be very useful for my organisation. His guidance and suggestions have been very valuable during the thesis period. I would like to express my indebtedness and sincere thanks to Prof. Sanjay G. Dhande for his valuable advice from time to time. It is with great pleasure, I thank Mr. Tarun Chaturvedi, Senior Project Associate and Mr. Awadhesh Kumar Singh, Project Associate, for their valuable and sincere help in my thesis completion. I am also thankful to all the members of CAD project laboratory for their co-operation and help in one way or another during the completion of the thesis work.

I am very much grateful to my wife, son and daughter for their patience and pains they have taken ,without a complaint, during my absence from home.

(Jai Narayan)

TABLE OF CONTENTS

List of figures

Nomenclature

Q_l : Rated volumetric flow to load @ rated pressure (m^3/sec)

Q_{vl} : Volumetric flow from/to spool end chamber(m^3/sec)

C_d : Coefficient of discharge of sharp edge orifice

x : Spool movement, Armature movement at center of the pole

x_{vm} : Maximum spool movement

rc : Radial clearance (m)

w : Port area gradient (m)

P_s : Supply pressure (MPa)

P_v : Valve pressure drop (MPa)

P_l : Load pressure drop (MPa)

ρ : Density of the fluid (Kgs / m^3)

μ : Dynamic viscosity of hydraulic fluid, Amplifier gain

K_q : Spool flow gain

K_c : Spool flow pressure coefficient

K_p : Spool pressure sensitivity coefficient

K_{q0} : Spool null flow gain

K_{c0} : Spool null flow pressure coefficient

K_{p0} : Spool null pressure sensitivity coefficient

Q_c : Center flow

u : Underlap, Velocity of jet at vena contracta

M_s : Mass of spool

M_f : Mass of fluid in spool chamber and nozzle

M_t : Total mass of fluid and spool

As : Spool end area

d : Minimum spool diameter

ds : Selected spool diameter

dr : Spool rod diameter

rs	: Spool land width
xs	: Distance between spool land
ls	: Spool length
v_{op}	: Volume at the end of spool
ω_{hf}	: Hydraulic natural frequency
ω_c	: Crossover frequency
K_{qu0}	: Spool null flow gain of underlap spool
K_{cu0}	: Spool null flow pressure coefficient of underlap spool
K_{pu0}	: Spool null pressure sensitivity coefficient of underlap spool
F_{1o}	: Flow force of outgoing fluid at port
F_{1i}	: Flow force of incoming fluid at port
F_1	: Total flow force
F_{2o}	: Transient force of outgoing fluid at port
F_{2i}	: Transient force of incoming fluid at port
F_2	: Total transient force
Ft	: Total fluid force
B_f	: Damping coefficient
K_f	: Flow force spring rate, Stiffness of feedback wire
K_{qp}	: Flow gain of pilot stage
P_{v1}, P_{v2}	: Nozzle back pressure (Pa)
P_{vl}	: Difference of the nozzle back pressure
ΔP_{vl}	: Change in net nozzle back pressure
Q_{vl}	: Flow to / from spool end chamber
C_{df}	: Discharge coefficient of nozzle flapper gap
C_{d0}	: Discharge coefficient fixed upstream orifice
d_n	: Nozzle diameter
a_n	: Nozzle area
A_0	: Area of the fixed upstream orifice
A_f	: Area of the curtain area of nozzle / flapper gap
x_{f0}	: Nozzle / flapper gap at neutral

x_f : Displacement of flapper at center of the nozzle(m)

β_e : Effective bulk modulus of the hydraulic fluid

ρ : Density of the fluid (Kgs/m ^{3})

d_0 : Diameter of the fixed stream orifice (m).

F_{n1} , F_{n2} : Force on flapper

T_d : Driving torque on the flapper (N.m)

r : Distance between Armature pivot & center of nozzle

b : Distance between center of nozzle & connecting point of spring to spool

K_f : Spring rate of feedback wire (Pa/m)

K_m : Magnetic spring constant of torque motor.

K_t : Torque constant of torque motor

K_a : Bending stiffness (angular) of flexure tube

E : Young's Modulus of feedback wire

A_g : Area of pole face (m ^{2})

R_1, R_2 : Reluctance of each gap

R_g : Reluctance of the air gap

J_a : Moment of inertia of armature/flapper

ω_{mf} : Natural frequency of torque motor (cps)

ω_{hf} : Natural frequency of spool

K_{vf} : Velocity coefficient

U_p : Magnetomotive force of permanent magnet (Ampere .Turn)

U_c : Magnetomotive force of control current (Ampere .Turn)

N_c : Number of turns in the coil

R_c : Coil resistance

r_p : Internal resistance of the coil

ϕ_a : Armature flux

ϕ_g : Permanent magnet flux

ϕ_c : Control current flux

ϕ_1 : Flux at gap 1

ϕ_2 : Flux at gap 2

Δi : Rated differential current

e_g : Signal voltage

g : Air gap at neutral

x : Armature movement at center of pole piece

μ_0 : Permeability of free space

θ : Armature rotation, Jet angle

B_a : Damping coefficient of armature

T_l : Load torque on armature

F : Magnetic force

I : Second moment of area of flexure tube

do : Outer diameter of flexure tube

di : Inner diameter of flexure tube

t : Flexure tube wall thickness

a : Armature length

L_t : Flexure tube length

K_{an} : Net spring rate of armature

K_{vf} : Velocity coefficient of servovalve

K_{qp} : Flow gain of pilot stage

Constants and their values:

P_v = 6.9 MPa

P_s = 20.7 MPa

C_d = 0.61

c_{d0} = 0.8

C_{df} = 0.64

β = 6.895×10^8 N/m^2

Viscosity(μ) = 1.224×10^{-2} $N.s/m^2$

Permeability of space (μ_0) = $4\pi \times 10^{-7}$ H/m

Radial clearance(rc) = 2×10^{-6} m

Density of hydraulic fluid (ρ) = 830 Kg / m^3

Density of steel = 7800 Kg / m^3

Specific resistance of wire = 1.73×10^{-8} Ω-m

Abstract

Hydraulic circuitry is widely used in machine tool applications, aircraft control systems, and similar operations because of such factors as positiveness, accuracy, flexibility, high power to weight ratio, fast starting, stopping and reversal with smoothness, precision and simplicity of the operations. Electrohydraulic valve forms an important element of the hydraulic servomechanism. In this report mathematical modeling and deign and analysis methodology of electrohydraulic servo valve has been developed. On the basis of the mathematical model, preliminary design parameters of a servovalve have been calculated and then system has been checked for stability. An application program has been developed using MATLAB software for the design and analysis of the servovalve.

Chapter 1
INTRODUCTION

1.1 Introduction

Hydraulic control is widely used in the field of power servomechanism such as auto pilot aircraft system, space vehicle control systems because of its light weight, positioning of machine tools, industrial robots, servo controlled vibration generator of vibration testing machine. Electrical devices are ideal for feedback measuring and for signal amplification and manipulation. Hydraulic actuators are ideally suited for power devices because of high power to weight ratio and compactness. The interface connection between electrical device and hydraulic devices in control systems is achieved by electrohydraulic servovalve. Electrohydraulic servovalve converts low power electrical signal into a motion of a valve which in turn control the flow and / or pressure to hydraulic actuator. Since large power is controlled by small and compact components, large torque to inertia ratio is realised and hence high speed of response is obtained.

Hydraulic control systems have its own merit and demerits. One of the problems is the nonlinear behavior of flow through orifices posing difficulties in the mathematical modeling. But the merits surpass the demerits. In this report design of a electrohydraulic servovalve has been taken up. The basic design criteria involved for design of various components have been presented and used for estimation of design parameters. More emphasis has been given to the design of mechanical components.

1.2 Types of servovalve

There are many types of servovalves. The types are classified on the basis of control mode, construction, types of spool position feedback, number of stages, types of pilot stage in multi-stage valve, types of torque motor, condition of spool lap with sleeve etc.. In the present work the design and analysis of flow control two- stage, nozzle/flapper position/forced feedback dry type servovalve has been taken up.

1.3 Configuration

The proposed configuration of the servovalve for the design will be similar to the one shown in Fig. 1.1. The typical servovalve consists of a steel body which houses a sleeve -spool, hydraulic amplifier and a torque motor integral with required oil filter inside the body. Thus the servovalve will have a torque motor, nozzle-flapper assembly and spool-sleeve assembly. The schematic arrangement is shown in the Fig 1.2. A brief description of the servovalve and its characteristics are given below. More details are available in the bibliographical references cited in the list references.

1.3.1 Brief Description and Operating Principle

The torque motor assembly consists of a permanent magnet, upper and lower pole pieces, armature and motor coils. A frictionless flexure tube and flapper is attached to the armature. The flapper movement placed in front of the nozzle forms the variable orifice. The torque motor is driven by the differential current input to the two coils that develops the torque approximately proportional to the input current on the armature which is mounted on the flexure tube and consequently produces angular displacement of the armature proportional to the input current. The flexure tube acts as restoring spring for the armature and is made up of a very thin metallic tube.

The pilot stage, which is nozzle flapper type, converts angular displacement of the torque motor armature to the unbalanced back pressure at the two nozzles to drive the spool. At the end of torque motor armature, the flapper is placed between two nozzles facing each other forms a variable orifice. The filtered hydraulic oil enters through variable orifice and impinges on both side of the flapper. Each nozzle is supplied with hydraulic supply pressure through fixed upstream orifice. The gap between the nozzle and flapper changes in accordance with the flapper deflection due to torque motor operation. Thus the restriction to the flow varies in accordance with the gap while the restriction of the fixed upstream orifice remain fixed. Then the back pressure of the nozzle which is the pressure of the intermediate chamber between the fixed upstream orifice and the nozzle varies according to the flapper deflection. The nozzle back pressure acts on the end surfaces of the spool to open the supply and load ports. Thus the pilot stage acts as hydraulic amplifier.

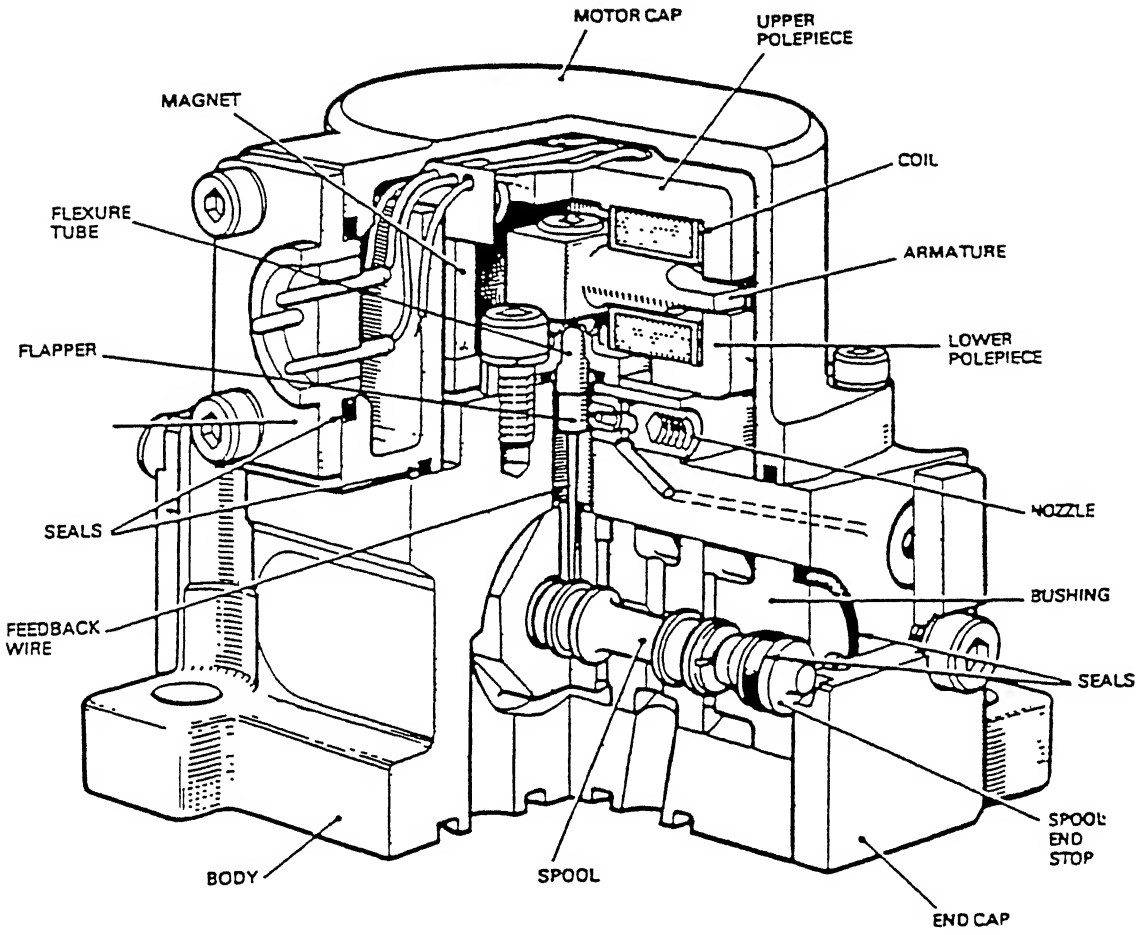

Fig. 1.1 Isometric view of servo valve

Courtesy of Dowty Boulton Paul Ltd, England

A simple cantelever spring having a rolling ball contact attached to flapper form a mechanical feedback arrangement. Two nozzles are provided on either side of this flapper. Rocking motion of the armature/flapper throttles the flow through one nozzle or the other.

The unbalanced nozzle back pressure caused by flapper deflection moves the spool in the corresponding direction. If, for example, the flapper deflects to the left, the left hand nozzle back pressure increases and the right-hand nozzle back pressure decreases, consequently the spool moves to the right. The feedback spring which connects the spool to the end of the torque motor armature is deflected by the spool. If the flapper deflects to the right, the spool moves to the left and the feedback spring deflects as shown in Fig. 1.3. Thus the feedback spring converts the spool position to a force signal which is fed back to the torque motor. Therefore, The spool moves to the position where the torque fed back by the feedback spring balances the torque due to the input current. Thus the spool position is proportional to the input current.

The valve body contains a spool which slides inside the sleeve The rectangular slots/holes in the sleeve and annular groove on the spool forms the port which connects supply and return pressures. Two service ports are also provided on the bottom of the body which also opens into the sleeve slots. Two end caps are provided on either side of the body to hold the spool and sleeve inside the body. The flow of the hydraulic fluid through a control orifice of the four-way spool valve is proportional to the opening of the orifice, that is, spool displacement. Therefore flow varies with the input current.

1.4 Materials

Following materials are generally used for the different parts of the servovalve :

Body, End caps & accessories	17-4 PH stainless steel
Spool & sleeve	AISI 440 C stainless steel
Filter	35μ sintered stainless steel wire mesh
Flexure tube	Berrylium copper
pole pieces and armature	4750 Nickel Iron Steel

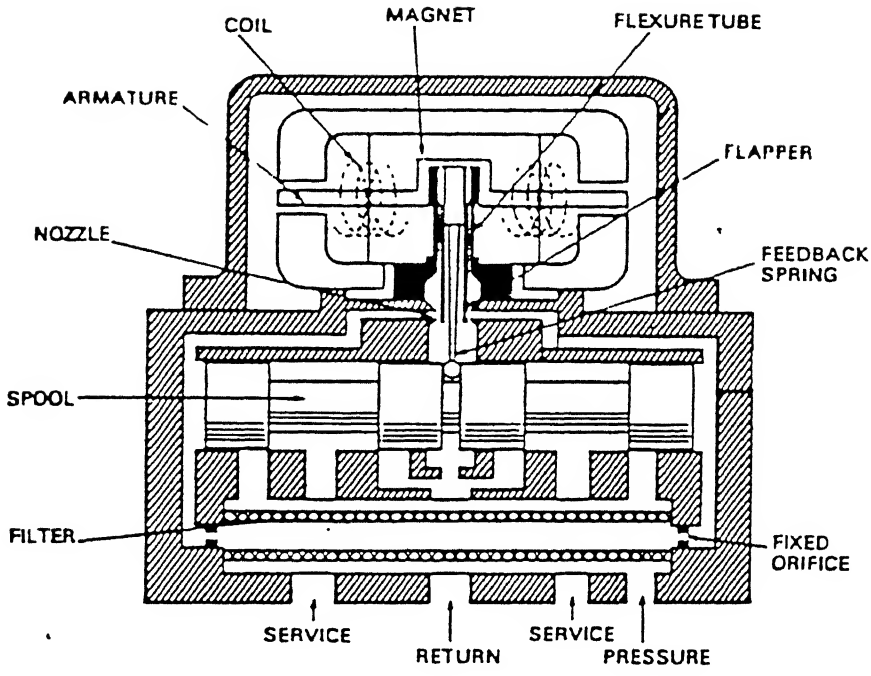

Fig. 1.2 Sectioned View of servo valve

Courtesy of Dowty Boulton Paul Ltd, England

Magnet	Alnico VI
Feed back wire	440 C Stainless steel
Torque motor cover	Anodised Aluminum alloy

1.5 Specification

For the design calculations, the following specifications have been used :

Rated flow	26 lpm	
supply pressure	20.7 MPa	
Hydraulic fluid	DTD 585 or MIL -H- 5606 or equivalent	
	Absolute viscosity	= 1.22×10^{-2} N-s /m^2
	Effective bulk modulus	= 6.895×10^{8} N/ m^2
	Density	= 830 Kgs/ m^3

1.6 Literature Survey

The electrohydraulic servovalve made its appearance in latter 1740s to satisfy aerospace needs for a fast response servo control system. Electrohydraulic servo system then in use were not significantly faster than electric servos. Servovalve were the slowest element in the control loop and system performances were limited because they were powered by small electric servos motors. In the early 1950s permanent magnet torque motors having fast response gained favour as a method of stroking valves and electrohydraulic servovalve took its present form [1].

Many researches have contributed the development of servovalve. Merritt [1] has contributed significantly in the design and analysis of servovalves. He has suggested various things as per his own experience and mentioned the gray areas. Though servovalves are manufactured and are available in the international market, reports on their detail design and analysis remain for internal circulation of the organisations. Yasusiro Oshima [4] has described principle, construction, performance and dynamic analysis. Guillon [3] has mentioned various kinds of servovalves manufactured by several firms. He has also elaborated the salient features of servovalves.

1.7 Objective

The objective is two fold:

1.7.1 Design Analysis

Design analysis including development of idealised (linearised) mathematical models involving some of the important parameters of the various stages (torque motor stage, flapper-nozzle stage and spool-valve stage).

(a) Spool / Sleeve Design

- Valve control port design, pressur drop and valve coefficients
- Spool stroke, driving force, null forces
- Spool lap design
- Valve dynamic forces and

(b) Hydraulic Amplifier Design

- Fixed upstream orifice
- Flapper
- Nozzle flapper opening orifice (variable orifice)
- Feed back wire stiffness

(c) Torque Motor Design

- No of coils and current rating
- Air gap and armature design
- Maximum torque analysis
- Magnet design for flux density and attractive force
- Coil impedance, rated current and quiescent current
- Flexure tube design

1.7.2 Performance Analysis

Performance analysis includes transient, steady-state, stability, frequency domain behaviour etc. They are:

- Transient response analysis
- Frequency response analysis for amplitude ratio and phase lag in the range of 5 Hz to 500 Hz
- Performance curve (Control flow v/s Load pressure drop)

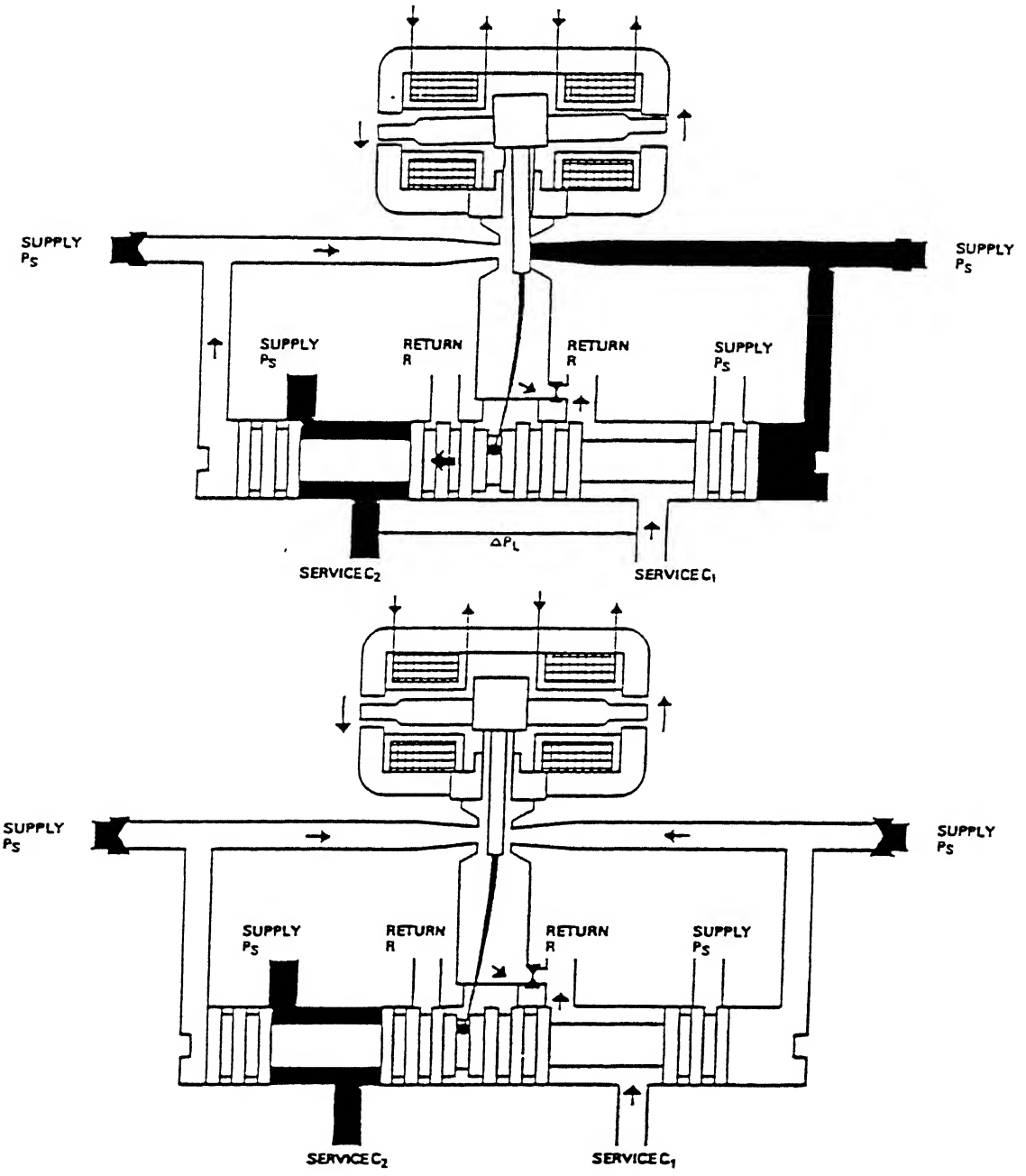

Fig. 1.3 Simplified schematic sectioned view

Courtesy of Dowty Boulton Paul Ltd, England

CHAPTER 2

Spool Valve

2.1 Spool valve design and analysis

The output stage of the servovalve is a four-way spool valve. Fig. 2.1 shows three-land four-way valve The spool valve can be defined in so many ways. With reference to the lap, the spool valve is classified as underlapped, zero lapped and overlapped spool valve.

An open center valve is one in which the width of the land is smaller than the width of port in the sleeve A zero lapped or critical center valve is one in which the land width is identical to the port width. An overlapped or closed centered valve is one in which the land width is greater than the port width. In this chapter zero-lap as well as underlap spool design analysis has been dealt with.

2.2 General Valve Analysis

2.2.1 Pressure flow characteristics

The pressure drop P_l across the load and the supply pressure P_s are important considerations The supply pressure has been selected as 20.7 MPa and load pressure drop to be two-third of the supply pressure for lower weight and maximum power transfer to the load [1].

The flow equation for the underlapped spool valve is as

$$Q_l = C_d w\,(u + x)\sqrt{\frac{P_s - P_l}{\rho}} - C_d\, w(u - x)\sqrt{\frac{P_s + P_l}{\rho}} \qquad (2\text{-}1)$$

This equation holds good within the underlapped region when $x < u$. Outside the underlapped region, only the first term or the second term of the right hand side of the Eq. (2-1) remains according to whether $x > u$ or $x < -u$ Eq. (2-1) can be rewritten as

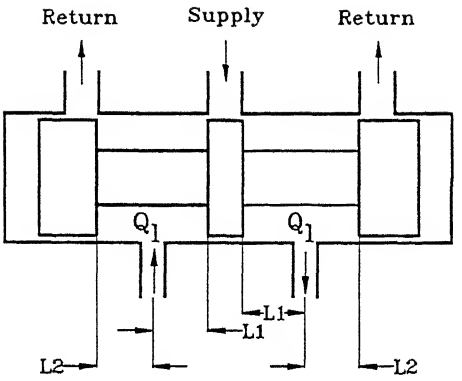

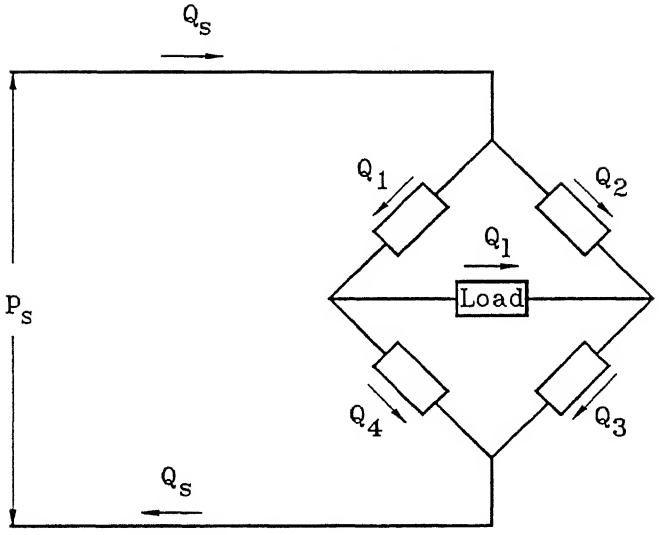

Fig. 2-1 Three-land-four-way spool valve

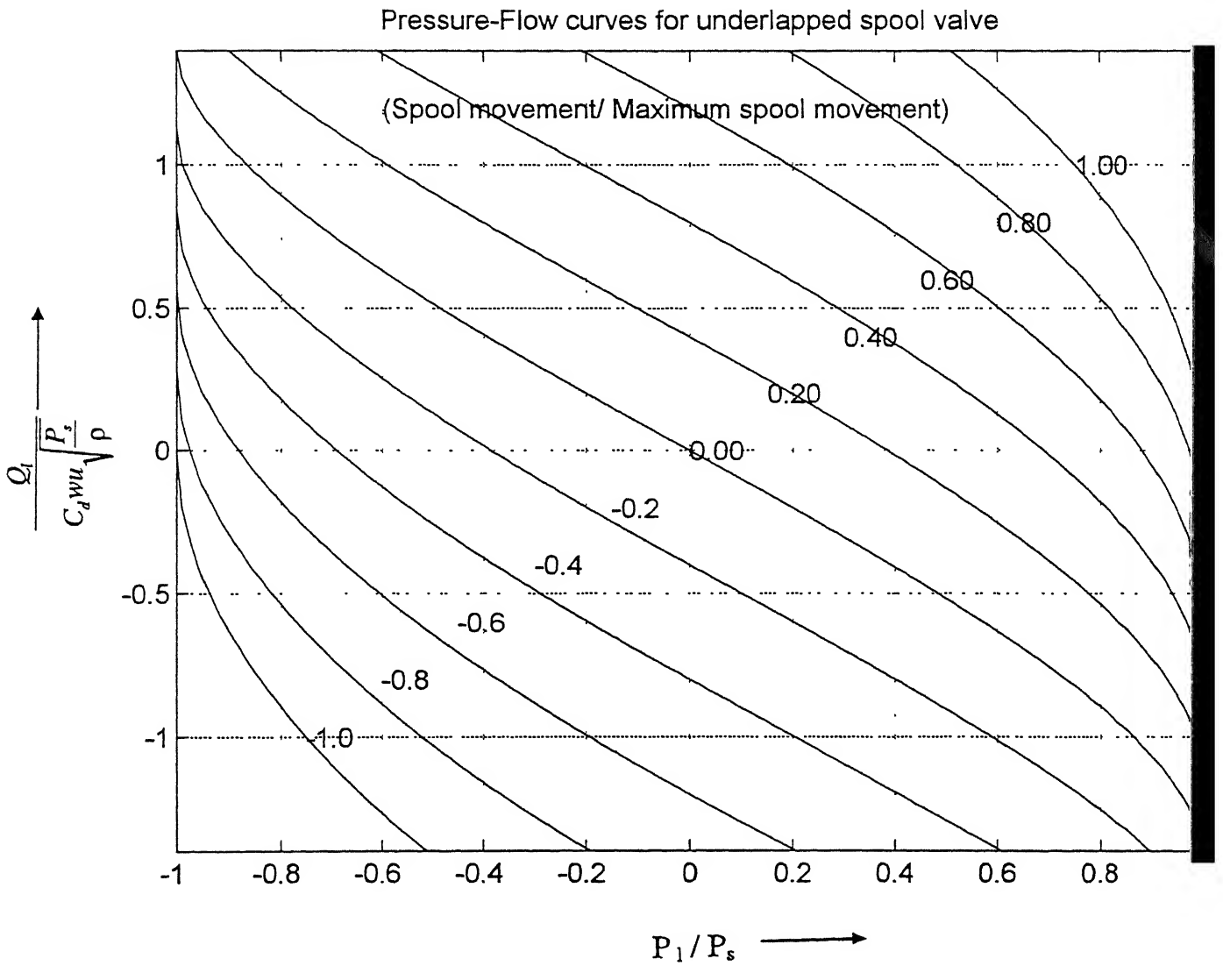

Fig. 2.2 Pressure flow characteristics of underlap spool valve

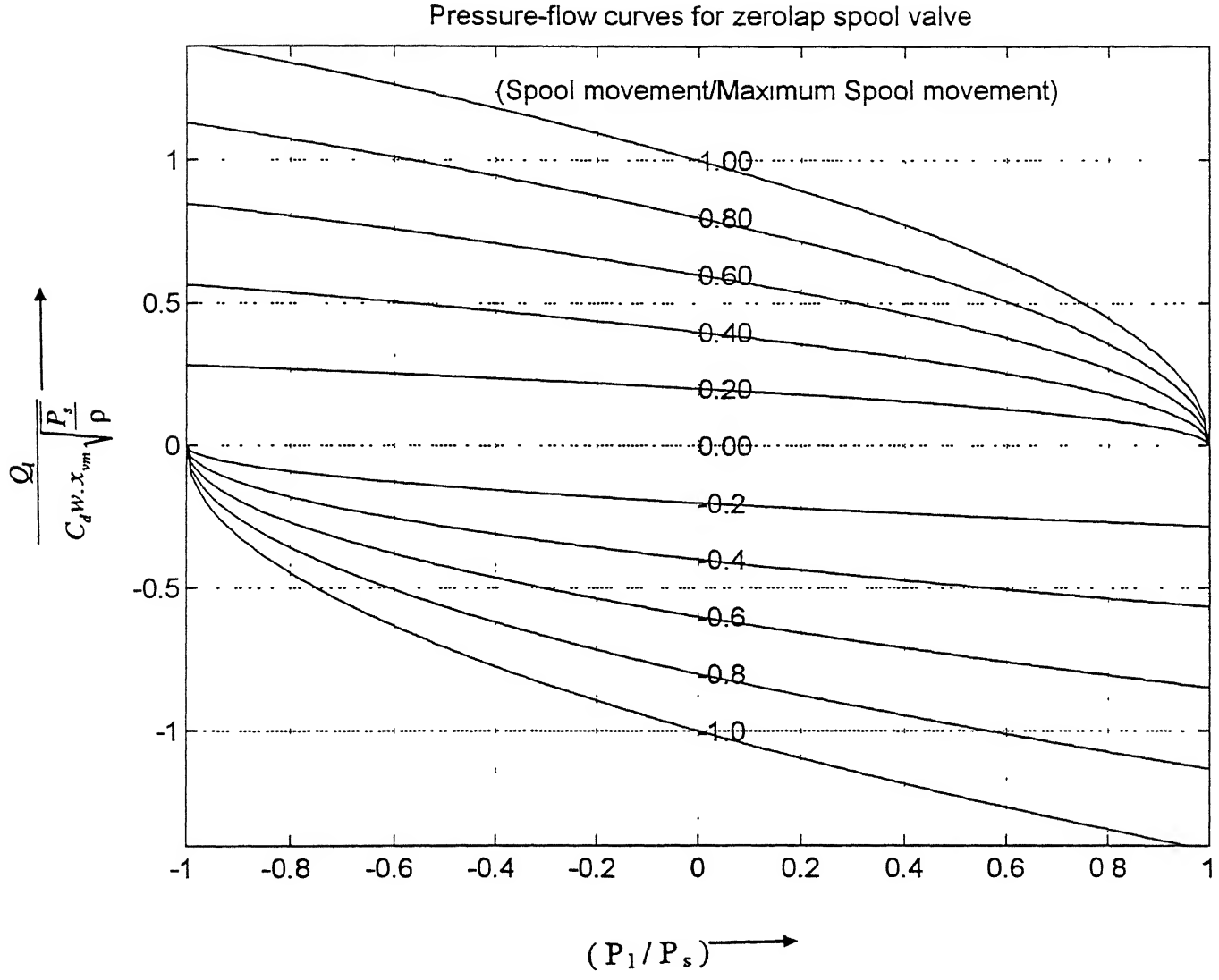

Fig. 2.3 Pressure flow characteristics of critical center spool valve

$$\frac{Q_l}{C_d w u\sqrt{\frac{P_s}{\rho}}} = (1+\frac{x}{u})\sqrt{1-\frac{P_l}{P_s}} - (1-\frac{x}{u})\sqrt{1+\frac{P_l}{P_s}} \qquad (2\text{-}2)$$

Where Q_l . Load flow

P_l : Pressure drop across the load

C_d : Discharge coefficient of orifice

x : Spool movement

u : Underlap

w : Area gradient of the port

ρ Density of the fluid

Plot of this equation is shown in the Fig. 2 2.

It is recognised that the pressure flow characteristics of underlapped valve are fairly linear within the underlapped region In the case of zero lapped valve, only the first term of the right hand side of the Eq. (2-1) remains When u = 0

$$Q_l = C_d w\, x\sqrt{\frac{P_s - P_l}{\rho}} \qquad (2\text{-}3)$$

Eq. (2-3) can be written as below for both positive as well as negative value of x

$$Q_l = C_d w x\sqrt{\frac{1}{\rho}(P_s - \frac{x\,P_l}{|x|}} \qquad (2\text{-}4)$$

Eq (2-4) is plotted in the normalised form as shown in the Fig 2 3. This figure shows that the pressure flow characteristics of zero lapped valve is considerably non-linear.

2.2.2 Valve coefficients

The non-linear equation can be linearised for dynamic analysis. In the case of zero lapped valve the linearised expression is·

$$\Delta Q_l = \frac{\partial Q_l}{\partial x}\,\Delta x + \frac{\partial Q_l}{\partial P_l}\,\Delta P_l \qquad (2\text{-}5)$$

Putting $K_q = \dfrac{\partial Q_l}{\partial x}$

and $K_c = -\dfrac{\partial Q_l}{\partial P_l}$

It can be shown that $\dfrac{\partial Q_l}{\partial P_l}$ is negative making K_c always positive.

Eq.(2-5) can be written as

$$\Delta Q_l = K_q.\Delta x - K_c \Delta P_l \qquad (2\text{-}6)$$

Where K_q is flow gain and K_c is flow pressure coefficient Flow gain is the most important of the characteristics of the servovalve Fig. 2.4 shows flow gain qualitatively for the three types of the spool centers The ratio of the K_q and K_c is defined as pressure sensitivity. Fig. 2.5 shows the pressure sensitivity curve [1]

$$K_p = \frac{\partial P_l}{\partial x} = -\frac{\partial Q_l / \partial x}{\partial Q_l / \partial p_l} \qquad \text{or} \quad K_p = \frac{k_q}{K_c} \qquad (2\text{-}7)$$

With these equations, the linearised equations becomes

$$\Delta Q_l = K_q.\Delta x - K_c \Delta P_l \qquad (2\text{-}8)$$

which is applicable to all types of the valves

The coefficients K_q, K_c and K_p are called valve coefficients and are extremely important in determining stability, frequency and other dynamic characteristics. The flow gain directly affects

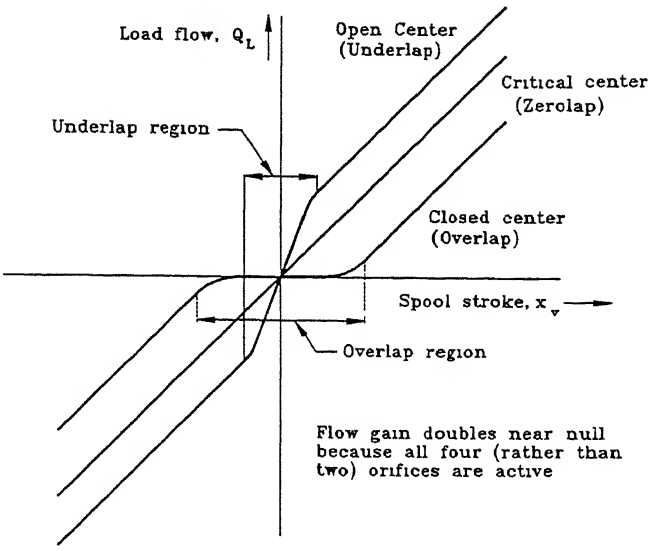

Fig. 2.4 Flow gain characteristics (different centers)

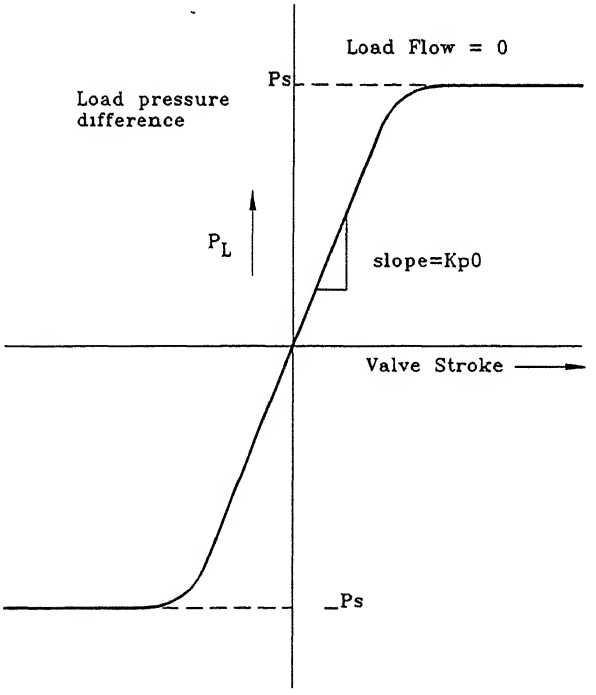

Block line pressure sensitivity curve

Fig. 2.5 Static Performances

the open loop gain constant in a system and, therefore, has a direct influence on system stability The flow pressure coefficient directly affect damping ratio of valve-motor combinations The pressure sensitivity of valve is quite large which accounts for the ability of the valve-motor combinations to breakaway large friction loads with little error.

The value of the valve coefficients vary with the operating point. The most important operating point is the origin of the pressure-flow curves (i e where $Q_l = P_l = x = 0$) because system operation usually occurs near this region, the valve flow gain is largest, giving high system gain. The flow-pressure coefficient is smallest giving a low damping ratio Hence this operating point is the most important and critical from stability point of view A stable system at this point is usually stable at all operating points The valve coefficients evaluated at this point are called the null valve coefficients

The valve coefficients for zero-lapped valve are obtained by partial differentiation of Eq (2-3) The resulting coefficients are as follows

$$K_q = C_d\, w \sqrt{\frac{P_s - P_l}{\rho}} \tag{2-9}$$

$$K_c = \frac{C_d . w . \sqrt{\dfrac{P_s - p_l}{\rho}}}{2\,(P_s - p_l)} \tag{2-10}$$

$$K_p = \frac{2(P_s - P_l)}{x} \tag{2-11}$$

The null coefficients are as follows

$$K_{q0} = C_d w \sqrt{\frac{P_s}{\rho}} \tag{2-12}$$

$$K_{c0} = 0 \tag{2-13}$$

$$K_{p0} = \infty \tag{2-14}$$

For a practical valve

$$K_{c0} = \frac{\pi w r c^2}{32\mu} \tag{2-15}$$

$$K_{p0} = \frac{32\mu C_d \sqrt{\frac{P_s}{\rho}}}{\pi c^2} \tag{2-16}$$

Where rc · Radial clearance between spool and sleeve

μ · Dynamic viscosity of the fluid

Null flow gain K_{q0} is a simple function of two well known and easily measurable quantities, that is, the valve area gradient and system supply pressure.

The null valve coefficients for underlapped spool valve can be obtained by differentiating the Eq (2-1) The null valve coefficients can be obtained by putting $Q_l = P_l = x = 0$

$$K_{qu0} = 2\, C_d w \sqrt{\frac{P_s}{\rho}} \tag{2-17}$$

$$K_{cu0} = \frac{C_d . w\, u \sqrt{\frac{P_s}{\rho}}}{P_s} \tag{2-18}$$

$$K_{pu0} = \frac{2\, P_s}{u} \tag{2-19}$$

K_{qu0}, K_{cu0} and K_{pu0} are null coefficients for underlap spool.

2.3 Leakage Characteristics

The ideal valve has perfect geometry so that the leakage flow is zero But ideal valve is difficult to manufacture The practical valve has radial clearances and minute underlap or overlap of the

order of 2 microns. It is the leakage characteristics which actually differentiates a practical valve from ideal valve

Let us assume that orifice are matched and symmetric And load flow lines are blocked (that is $Q_l = 0$) By stroking the valve and recording the load pressure P_l and total supply flow Q_s (which is actually leakage flow since load flow is zero) for a given supply pressure and plotting the results as shown in the Fig. 2.6 and Fig 2.6(a) schematically The load pressure P_l quickly increases to supply pressure after very small spool displacement. The leakage flow is maximum at valve neutral and decreases rapidly with valve stroke when the spool is centered, the total supply through the valve known as center flow

The center flow equation for critical center valve

$$Q_c = \frac{\pi . w\, rc^2\, P_s}{32\, \mu} \tag{2-20}$$

and center flow for underlap spool

$$Q_c = 2\, C_d\, w\, u . \sqrt{\frac{P_s}{\rho}} \tag{2-21}$$

2.4 Stroking Force

2.4.1 Flow force

In the spool valve, the fluid flowing in the valve chamber and through the valve orifice creates force acting on the spool in the axial as well as transverse direction. Axial force consists of steady -state force and transient force Fig. 2.7 shows the pattern of the fluid flow in valve chamber and through valve orifice. As shown in the Fig 2 7, only two orifices are active at a time in an ideal critical center valve. The fluid enters through one port and goes out through another in the form of a jet making angle θ with the axial direction. Von Mises conducted experiments and it was found that for the negligible radial clearance the jet angle θ was 69° [1,4]. The jet going out with such an angle give rise to reaction force due to efflux of the momentum. The force on the spool due to outgoing fluid in axial direction can be written as:

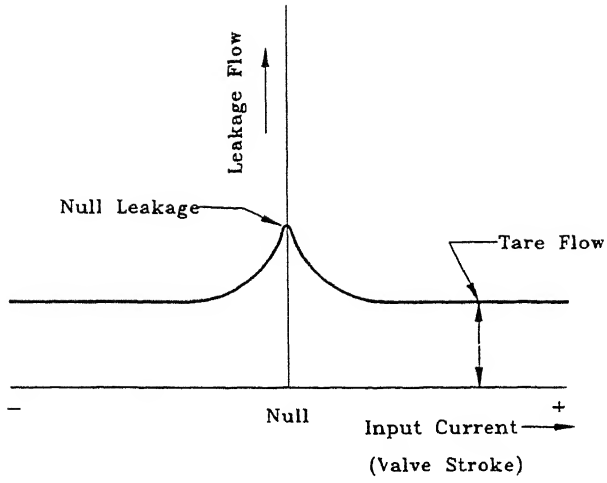

Fig. 2.6 Typical internal leakage curve

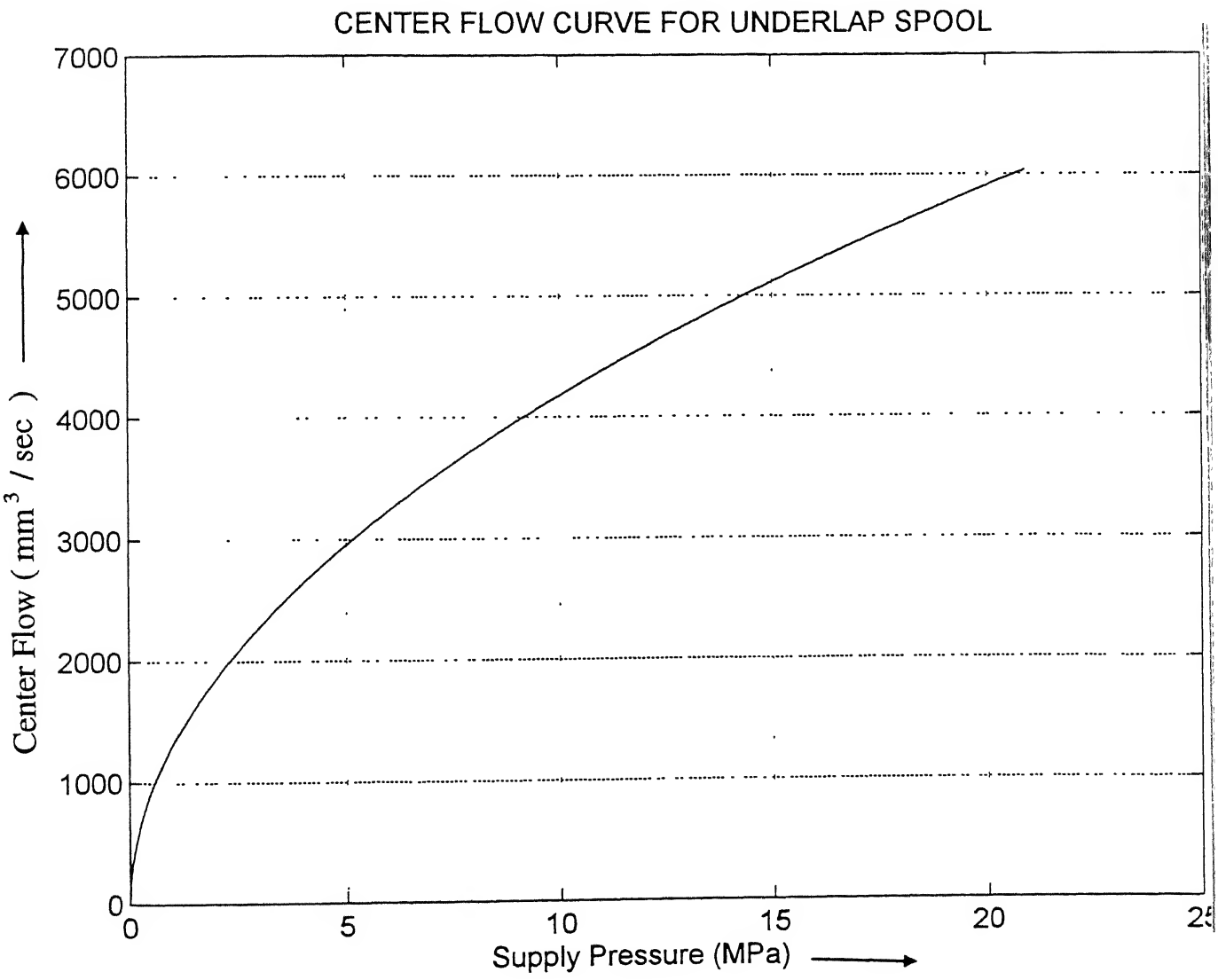

Fig 2.6a Leakage flow v/s supply pressure

$$F_{10} = Q\rho v\cos\theta \tag{2-22}$$

where Q . Volumetric flow rate

v Velocity of jet at Vena contracta

by Bernoulli's equation we know

$$v = \sqrt{\frac{2}{\rho}\Delta P} \tag{2-23}$$

where ΔP = Pressure difference across the metering orifice The flow rate is

$$Q = C_d w x\sqrt{\frac{2}{\rho}\Delta P} \tag{2-24}$$

Substituting Eq (2-23) and (2-24) in Eq.(2-22) we get

$$F_{10} = 2\ C_d\ w\ x\ \cos\theta\ \Delta P \tag{2-25}$$

Where F_{10} . Axial force due to out going jet

The direction of the force is such that it tends to close the valve orifice. This means that the steady -state axial force acts on the spool as a restoring force In actual valve there are two identical orifices in series At another metering orifice, the jet comes in the annular valve chamber from the load In this case, the steady-state axial force is of the form given in Eq. (2-25). When the valve is symmetrical, the steady-state axial force acting on the spool works out to be :

$$F_1 = F_{10} + f_{1i} = 2\ C_d\ w\ x\ (P_s - P_l)\ \cos\theta \tag{2-26}$$

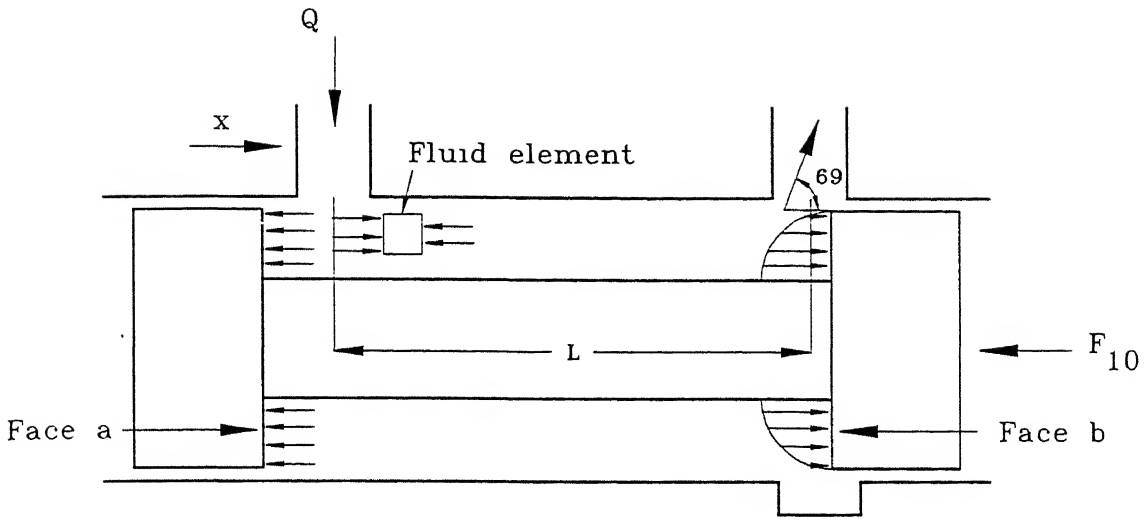

Fig. 2.7 Flow force on a spool valve

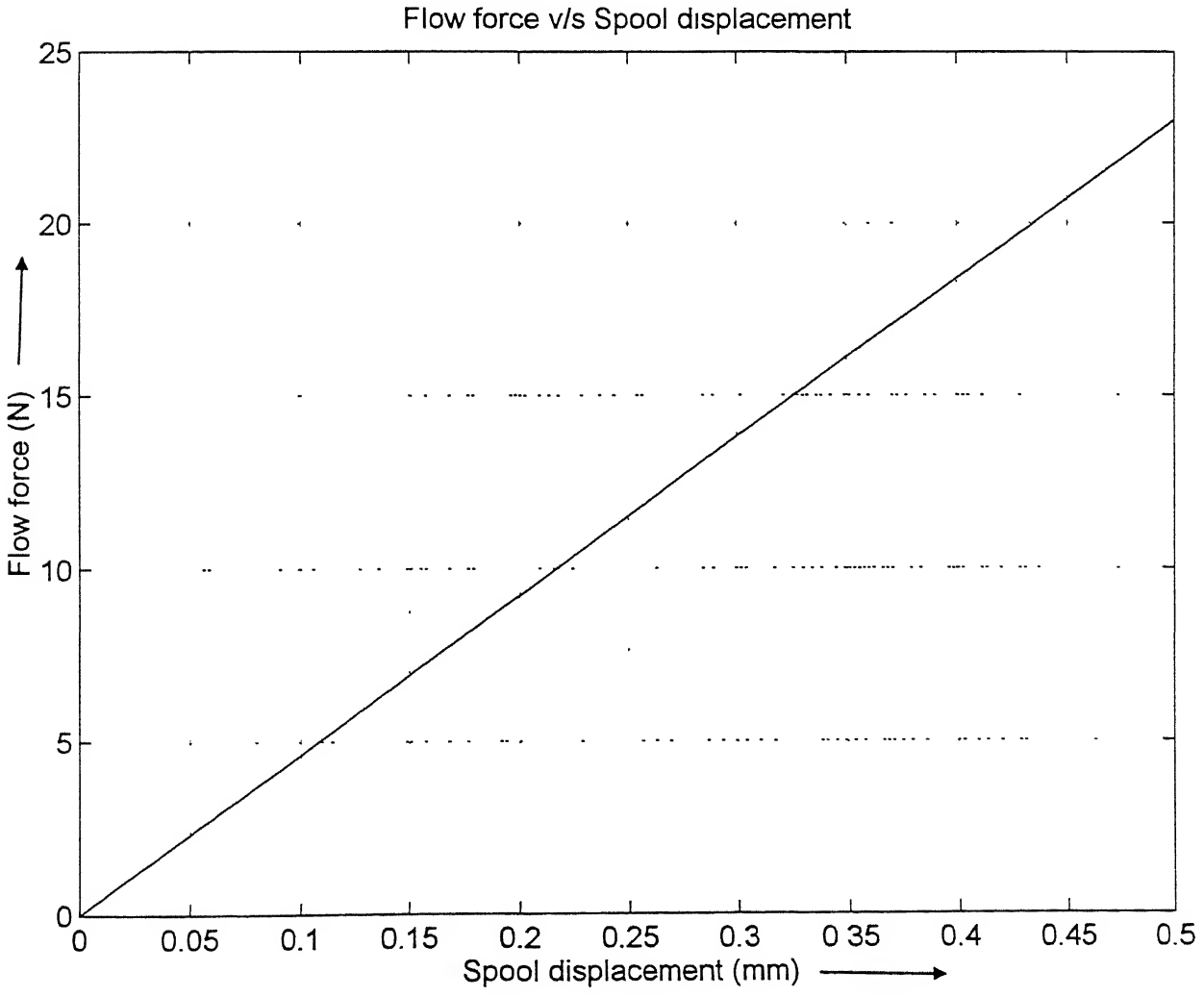

Fig. 2.8 Flow force v/s spool movement

The steady-state flow force is a significant contributor to the force required to stroke the spool valves The flow force compensation method have been covered in [1]

2.4.2 Transient Force

When the fluid in the valve chamber is accelerated, the transient axial force F_2 is produced The transient axial force due to outgoing fluid is given as

$$F_{20} = M_f a = \rho L_2 A_v \frac{d\left(Q/A_v\right)}{dt} = \rho L_2 \frac{dQ}{dt} \tag{2-27}$$

Where M_f · Mass of the fluid in one spool/sleeve chamber

a Acceleration of the fluid

L_2 Distance between centers of incoming and outgoing flows as

A_v Area of spool land

substituting for Q in Eq.(3-27) we get

$$F_{20} = L_2 C_d w \sqrt{2\rho\Delta p}\frac{dx}{dt} + \frac{L_2 C_d w x}{\sqrt{\frac{2}{\rho}\Delta P}}\frac{d(\Delta P)}{dt} \tag{2-28}$$

The pressure derivative d(ΔP)/dt term is neglected because it does not play any significant role in valve performance [1]. Eq. (2-28) can be written as

$$F_{20} = L_2 C_d w \sqrt{2\rho\Delta p}\frac{dx}{dt} \tag{2-29}$$

The direction of this force is such that it tends to close the valve orifice. However the direction of the transient axial force due to incoming jet is opposite The transient force due to incoming jet becomes

$$F_{2t} = -L_1 C_d \sqrt{2\rho\Delta P}\frac{dx}{dt} \tag{2-30}$$

Therefore the transient axial force F_2 is

$$F_2 = F_{20} + F_{2t} = (L_2 - L_1)C_d w\sqrt{2\rho\Delta P}\frac{dx}{dt} = LC_d w\sqrt{\rho(P_s - P_l)}\frac{dx}{dt} \tag{2-31}$$

Where $L=(L_2 - L_1)$ is damping length. If $L > 0$ the transient axial force is stabilising. For $L<0$ the transient axial force is destabilising. Therefore valve should be designed so that $L_2 \geq L_1$ to prevent instability

Combining the steady - state axial force and transient axial force, the total axial force F_t is

$$F_t = 2C_d w Cos\theta(P_s - P_l)x + (L_2 - L_1)C_d w\sqrt{\rho(P_s - P_l)}\frac{dx}{dt} \tag{2-32}$$

2.5 Dynamic Analysis

The equation of the motion of spool can be written as

$$F_t = M_s\frac{d^2x}{dt^2} + B_f\frac{dx}{dt} + K_s x \tag{2-33}$$

Where M_s : Mass of the spool (Kg)

B_f : Damping coefficient due to transient flow force (N-sec/m)

K_s : Flow force spring rate

Comparing Eq.(2-32) and (2-33) we get

$$B_f = (L_2 - L_1)C_d w\sqrt{\rho(P_s - P_l)} \tag{2-34}$$

and

$$K_s = 2C_d w Cos\theta(P_s - P_l) \tag{2-35}$$

Thus we see that the steady -state flow force acts as a centering spring on the valve and the transient flow force behave like a viscous damping.

Similarly, damping coefficient and flow force spring rate for underlap valve can be derived. The final equation is as follows·

$$B_f = 2(L_2 - L_1)C_d w\sqrt{\rho(P_s - P_l)} \tag{2-36}$$

and

$$K_s = 4C_d w Cos\theta(P_s - P_l) \tag{2-37}$$

As with critical center valve, steady-state flow force acts as a centering spring and transient flow force acts as viscous damping. However it is found that both the spring rate and viscous damping coefficients for underlap spool valve are twice that of a critical center spool valve.

2.6 Frequency Response analysis

Laplace Transforming the Eq (2-33) and after rearranging we get the equation for transfer function as

$$\frac{x(s)}{F(s)} = \frac{1}{M_s s^2 + B_f s + K_s} \tag{2-38}$$

where K_s Flow force spring rate (N/m)

Eq (2-38) has been analysed using the MATLAB software with the data generated for the preliminary spool. The Plot is shown in the Fig. 2.9 The Fig 2.9 shows that the natural frequency is above 400 Hz and the gain is constant upto 200 Hz (approx) without any phase difference. The natural frequency and phase depends on the system parameters

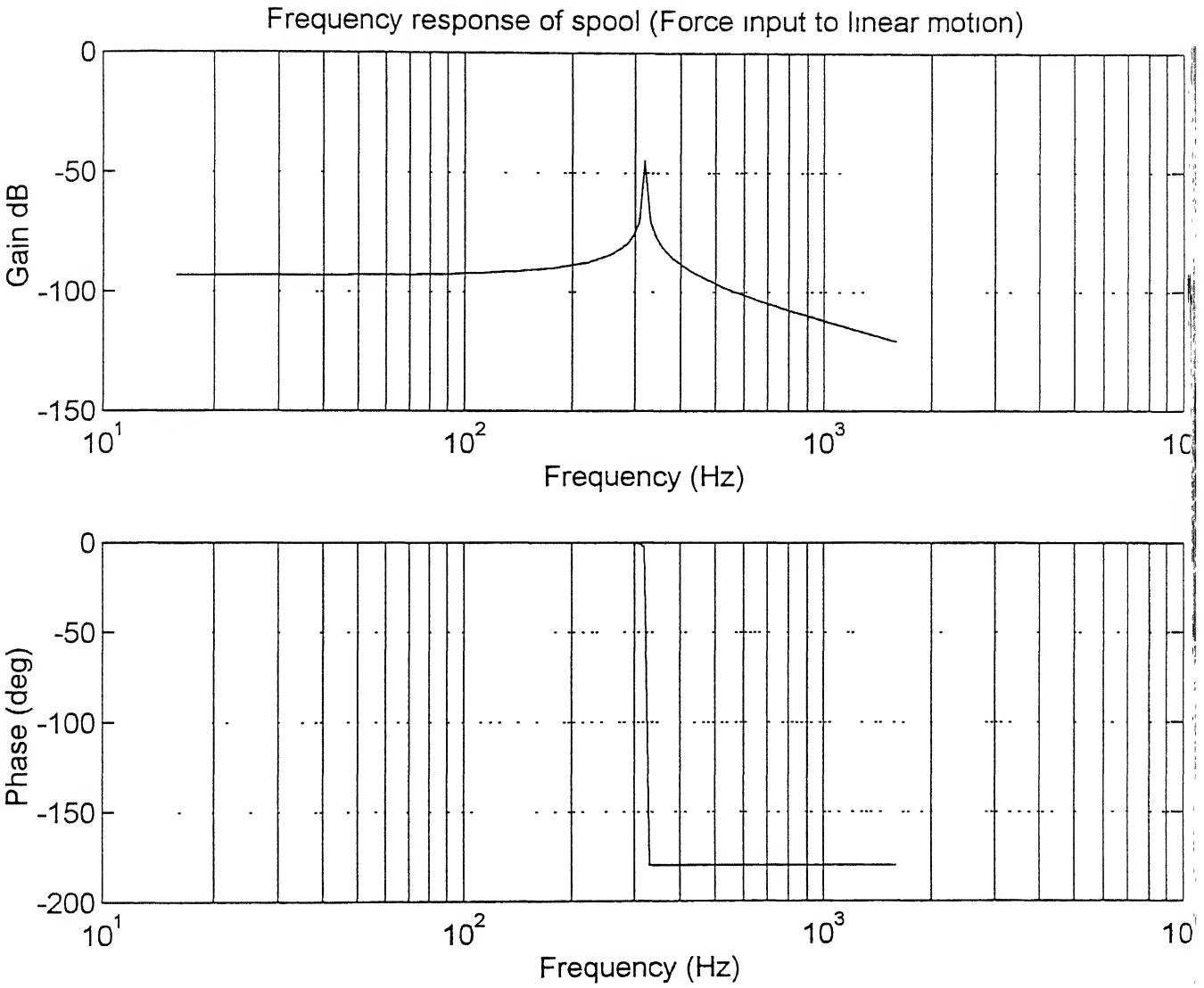

Fig. 2.9 Frequency response plot of spool

Chapter 3

Nozzle Flapper Hydraulic Amplifier

3.1 Hydraulic Amplifier Requirement

As we have seen in the previous chapter that flow force on the spool is of sizable value. Experimentally it was found that flow force was nearly twice of the theoretical one [1] So the source stroking the spool should have force capability in excess of the flow force to stroke the spool and to shear the dirt particles which might lodge in the orifices.

Flow force are normally quite large and are the major contributor to the total force required to stroke the spool valve Several compensation schemes to reduce or eliminate such flow forces have been investigated but non have met with general acceptance because of manufacturing cost and the non-linear flow force which results from the imperfect compensation The practical solution to this problem has been the two stage servovalve in which hydraulic first stage, usually flapper valve provides quite an adequate force to stroke the second stage spool valve.

Nearly all two-stage servo valves have a flapper valve first stage which constitute their major application. The pressure flow curves of flapper valves are relatively linear and performance are quite predictable and dependable. The purpose of this section is to derive the equations for null coefficients, flow forces for double jet configuration and to develop relations for design

3.2 Nozzle Flapper Valve Analysis

Schematic arrangement of the double jet nozzle flapper is shown in the Fig 3-1
In this figure

P_{v1}, P_{v2} · Nozzle back pressures

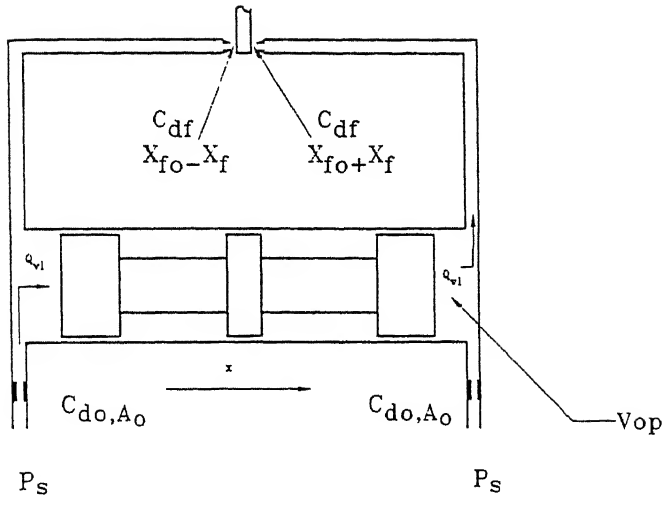

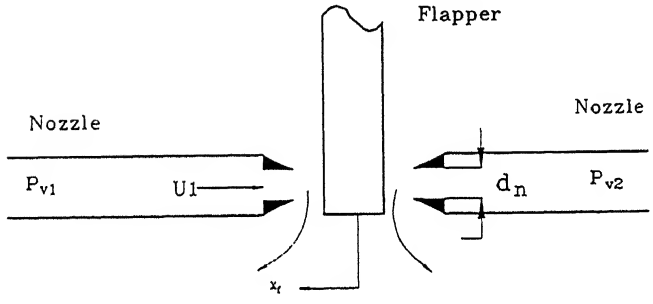

Fig. 3.1 Nozzle flapper pilot stage

q_{vl} : Volumetric flow coming into or going out from spool end chamber

C_{df} Discharge coefficient of nozzle flapper gap

C_{d0} : Discharge coeff. of fixed upstream orifice

d_n : Nozzle diameter

A_f · Area of the flapper curtain area

A_0 : Area of fixed upstream orifice

a_n . Area of the nozzle

x_f Displacement of flapper at center of the nozzle from equilibrium position

x_{f0} Nozzle flapper gap at neutral

The fixed upstream orifices are used to cause a control pressure P_{v1} or P_{v2} which can be modulated by moving the flapper At the flapper, the curtain area rather than the nozzle area is the controlling restriction.

At the no load flow the back pressure is give by:

$$\frac{P_{v1}}{P_s} = \left[1 + \left(\frac{C_{df}A_f}{C_{d0}A_0}\right)^2\right]^{-1} \tag{3-1}$$

The plot of this curve is shown in the Fig. 3-2. The maximum pressure sensitivity occurs when $P_{v1} = 0.5\ P_s$ Therefore, an equilibrium control pressure of $0\ 5\ P_s$ is considered as a design criteria. This criteria requires that the orifice ratio at the null point be equal to unity, that is,

$$\frac{C_{df}A_f}{C_{d0}A_0} = \frac{C_{df}\pi d_n x_{f0}}{C_{d0}A_0} = 1 \tag{3-2}$$

The flow equations are :

$$q_{vl} = C_{d0}A_0\sqrt{\frac{2(P_s - P_{v1})}{\rho}} - C_{df}\pi.d_n\,(x_{f0} - x_f)\sqrt{\frac{2.p_{v1}}{\rho}} \tag{3-3}$$

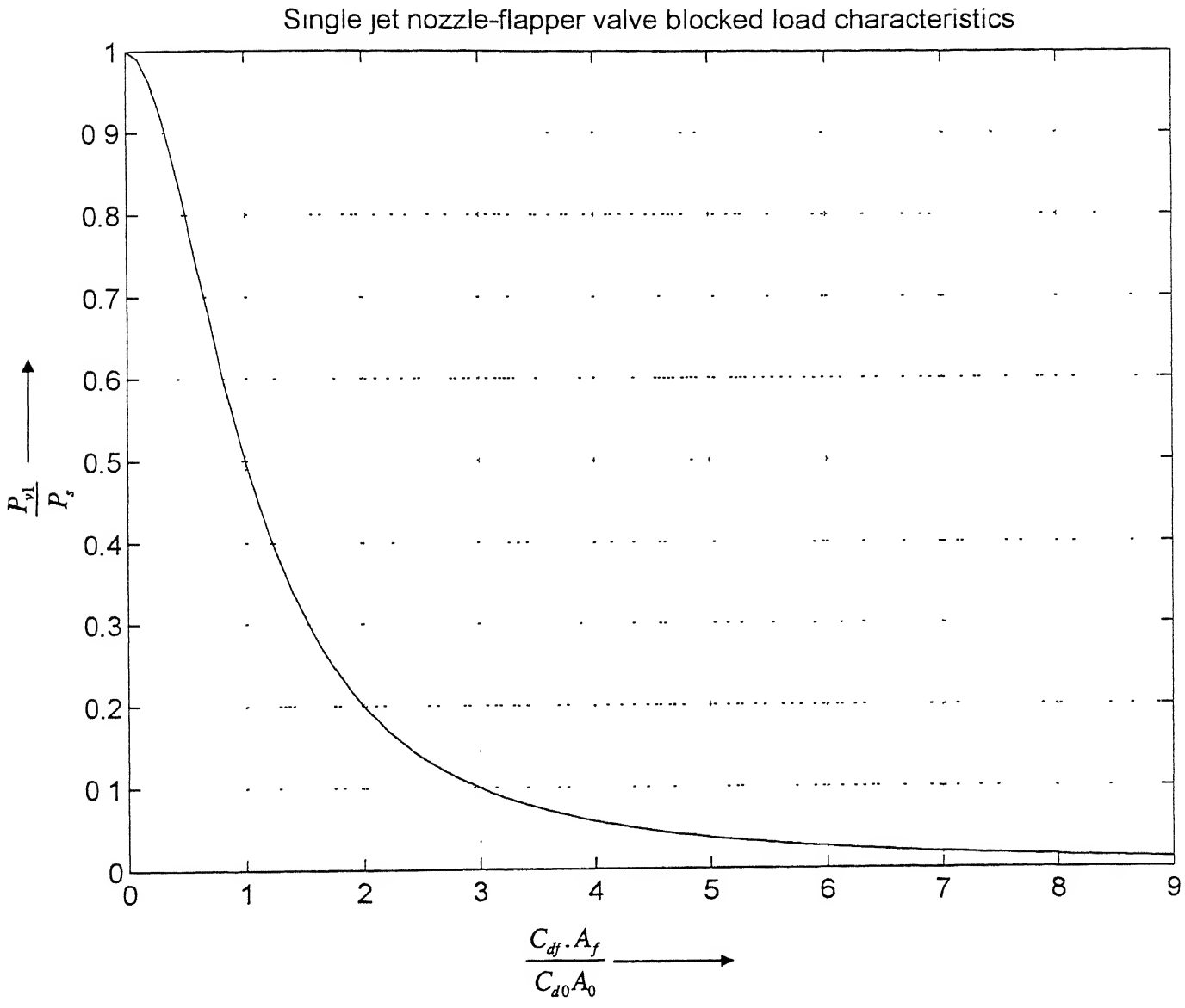

Fig. 3.2 Blocked load characteristics of single jet flapper

$$q_{vl} = C_{df}.\pi.d_n\,(x_{f0} + x_f)\sqrt{\frac{2.P_{vl}}{\rho}} - C_{df}A_0\sqrt{\frac{2}{\rho}(P_s - P_{vl})} \tag{3-4}$$

The leakage or center flow at null is given by

$$q_c = 2.C_{df}\pi.d_n x_{f0}\left(\frac{P_s}{\rho}\right)^{1/2} \tag{3-5}$$

Eq. (3-1) and (3-2) can be linearised as

$$\Delta q_{vl} = C_{df}\pi.d_n\sqrt{\frac{P_s}{\rho}}\Delta x_f - \frac{2\,C_{df}\pi\,d_n.x_f}{\sqrt{\rho.P_s}}\Delta P_{vl} \tag{3-6}$$

and

$$\Delta q_{vl} = C_{df}.\pi\,d_n\sqrt{\frac{P_s}{\rho}}\Delta x_f + \frac{2.C_{df}\pi.d_n x_f}{\sqrt{\rho.P_s}}\Delta P_{v2} \tag{3-7}$$

Adding Eq (3-6) and (3-7) and using $P_{vl} = P_{v1} - P_{v2}$

We get

$$\Delta q_{vl} = K_{q0}\,\Delta x_f - K_{c0}\,\Delta P_{v1} \tag{3-8}$$

where

$$K_{q0} = C_{df}.\pi.d_n\sqrt{\frac{P_s}{\rho}} \tag{3-9}$$

$$K_{c0} = \frac{C_{df}\pi.d_n x_f}{\sqrt{\rho P_s}} \tag{3-10}$$

K_{q0} and K_{c0} are null flow gain and null pressure coefficients for flapper. The ratio of the two gives pressure sensitivity K_{p0} which is given by

$$K_{p0} = \frac{P_s}{x_{f0}} \tag{3-11}$$

3.3 Flow force on the flapper

The flow force of the jet acting on the flapper which produces a load torque on the torque motor armature. The flow force of the left hand jet is given by:

$$F_{n1} = (P_{v1} + \frac{1}{2}\rho U_1^2)a_n \tag{3-12}$$

where U_1 is the fluid velocity at the plane of nozzle end and a_n is the area of the nozzle. We can write

$$U_1 = \frac{1}{d_n} 4C_{df}(x_{f0} - x_f)\sqrt{\frac{2}{\rho}P_{v1}} \tag{3-13}$$

Substituting Eq.(3-12) in (3-11), we obtain

$$F_{n1} = P_{v1}\left[1 + \frac{16C_{df}^{\ 2}\left(x_{f0} - x_f\right)^2}{d_n^{\ 2}}\right]a_n \tag{3-14}$$

similarly we can write the flow force F_{n2} of the right hand side as

$$F_{n1} = P_{v1}\left[1 + \frac{16C_{df}^{\ 2}\left(x_{f0} + x_f\right)^2}{d_n^{\ 2}}\right]a_n \tag{3-15}$$

The net flow force on the flapper is given by the difference of Eq. (3-13) and (3-14) which on simplification and by using $P_{v1} \approx P_{v2} \approx P_s/2$ and $P_{v1} = P_{v1} - P_{v2}$ we obtain

$$F_{n1} - F_{n2} = P_{vl}a_n + 4\pi C_{df}^2 x_{f0} P_{vl} + 4\pi C_{df}^2 x_f^2 P_{vl} - 8\pi C_{df}^2 x_{f0} P_s x_f \qquad (3\text{-}16)$$

For the actual nozzle flapper design the second and third terms can be neglected because x_f and x_{f0} are negligible compared with a_n and P_{vl} is far smaller than P_s. Hence we can write

$$F_{n1} - F_{n2} = P_{vl}.a_n - 8\pi C_{df}^2 x_{f0} P_s x_f \qquad (3\text{-}17)$$

The plot of the net flow force on the flapper as a function of flapper displacement is shown in the Fig. 3 3.

3.4 Dynamic analysis

The equation of motion of the flapper can be written as

$$T_d = J_a \frac{d^2\theta}{dt^2} + K_a\theta + (F_{n1} - F_{n2})r \qquad (3\text{-}18)$$

Where T_d is the driving torque on the flapper such as that which would be obtained from a torque motor For small angles

$$\tan\theta = \frac{x_f}{r} \approx \theta \qquad (3\text{-}19)$$

Where r Distance between nozzle center and armature center

θ : Armature rotation(radian)

Substituting Eq. (3-17) and (3-19) in Eq. (3-18) we get

$$T_d = \frac{J_a}{r}\frac{d^2x_f}{dt^2} + rP_{vl}a_n + \left[\frac{K_a}{r^2} - (8\pi C_{df} P_s x_{f0})\right] r x_f \qquad (3\text{-}20)$$

Thus flow force due to fluid impingement on the flapper acts as negative spring on the flapper. From Eq (3-20) it is also clear that the stiffness of the source driving the flapper

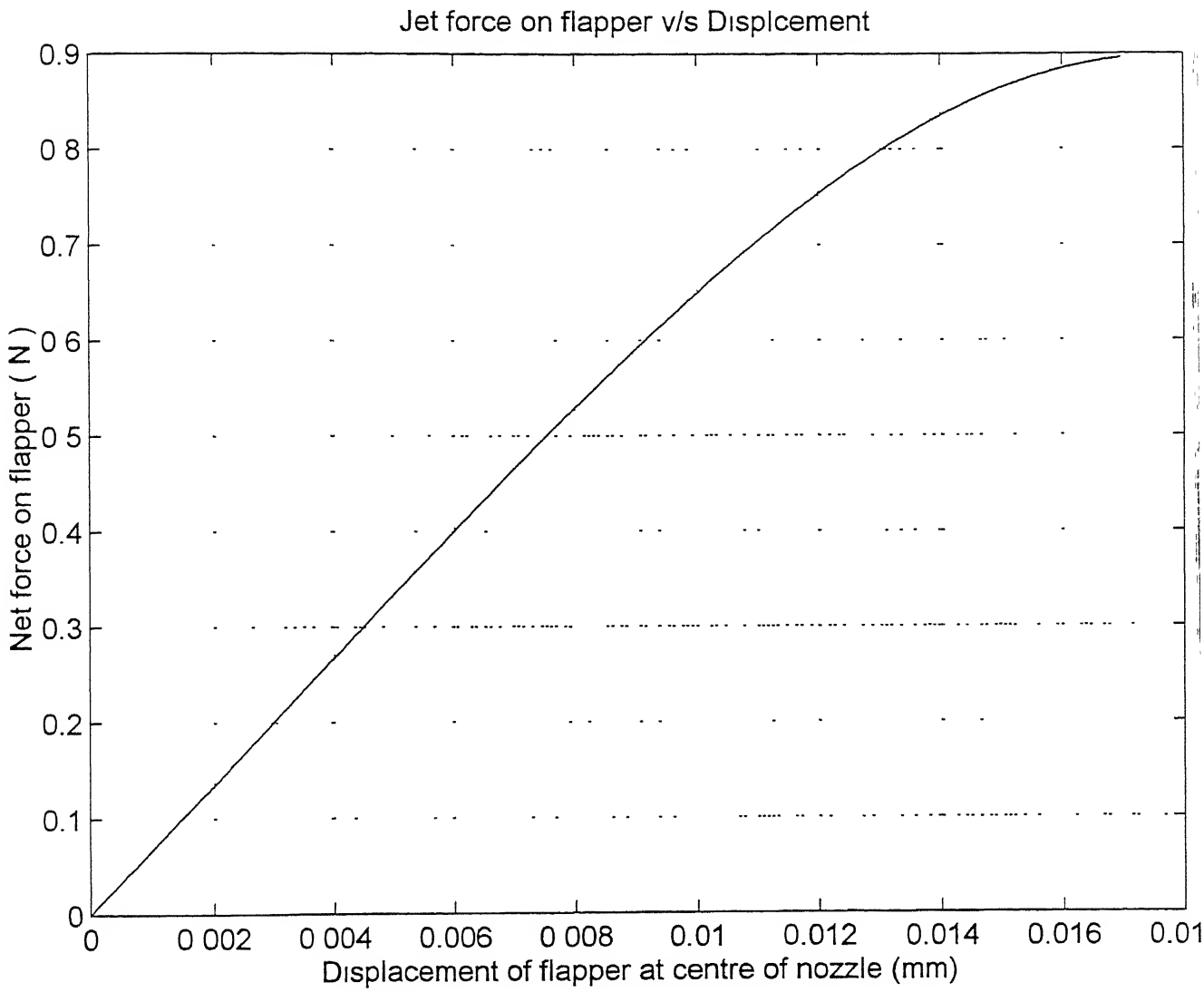

Fig. 3.3 Net force on flapper

must be greater than the negative spring rate to prevent the possibility of flapper instability. However overall stability must be determined from the analysis of the system in which the valve is placed

3.4.1 Frequency response plot

Taking Laplace Transform of Eq. (3-20) and after simplification we get the Transfer Function as

$$\frac{x_f(s)}{T_d(s)} = \frac{r}{J_a s^2 + (K_a - 8\pi r^2 C_{df}^2 P_s x_{f0})} \tag{3-21}$$

J_a Moment of inertia of armature /flapper (Kg - m ^{2})

K_a Spring constant of flexure tube (explained in next chapter N-m/ rad)

Frequency response plot of Eq.(3-21) has been generated using MATLAB software. The plot is shown in the Fig 3-4. From this figure it is clear that the natural frequency of the flapper is above 100 Hz and gain remain constant upto 100 Hz.

3.5 Spool stroking force

The differential pressure at end of the spool generates the spool stoking force. This force moves the spool which opens the load port to pass the fluid. The spool force is given by

$$F_s = P_{vl} A_s \tag{3-22}$$

The plot of the spool force as a function of flapper movement is shown in Fig 3.5. The spool stroking force increases as flapper movement upto certain value Then the force saturates. For the design parameters computed, it shows that the spool force is approximately 700 N

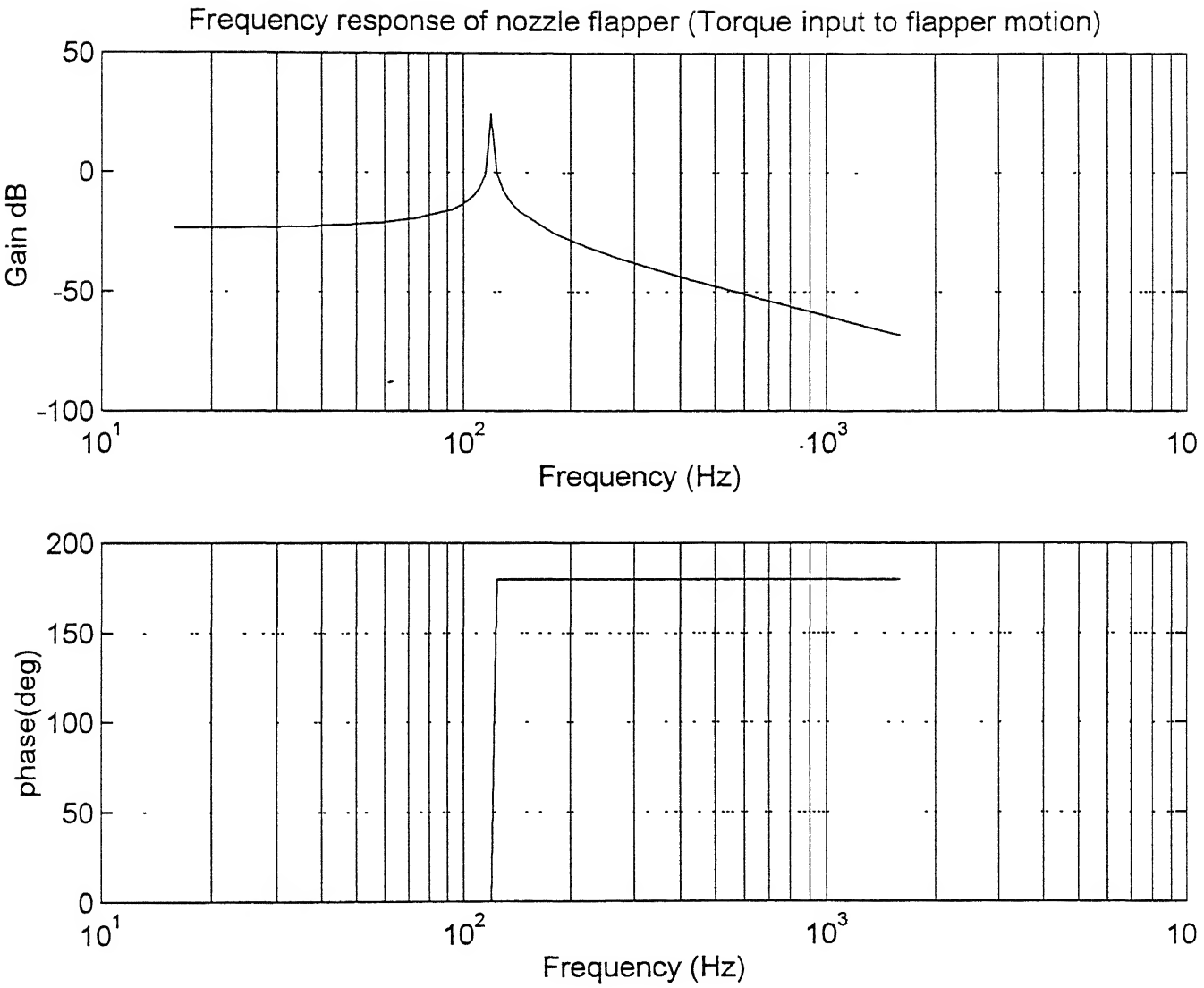

Fig. 3.4 Frequency response plot of nozzle flapper

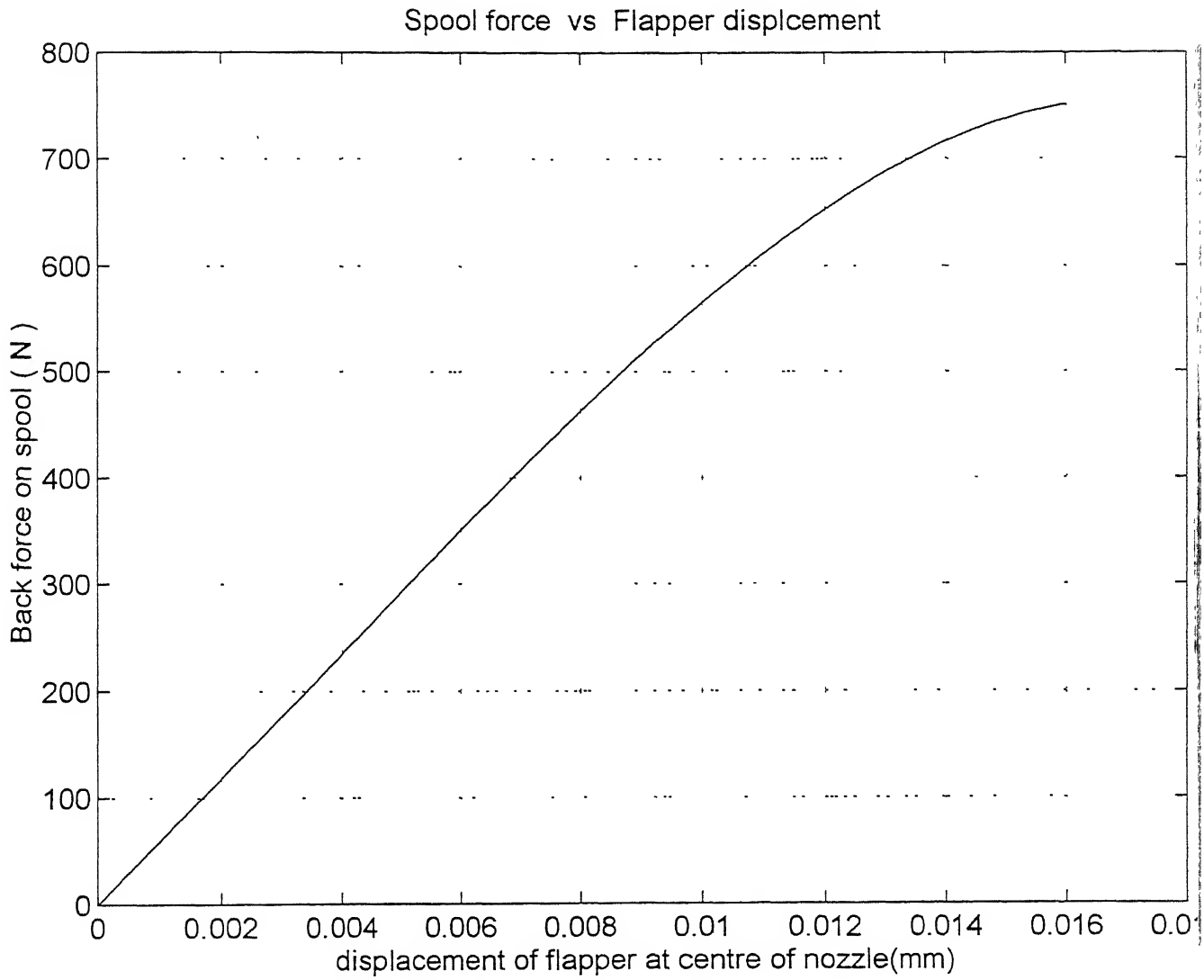

Fig. 3.5 Spool stroking force

Chapter 4

Permanent Magnet Torque Motor Design and Analysis

4.1 Description

Permanent magnet torque motor are the most widely used electromechanical devices for the stroking of the servovalves using an electrical signal. The permanent magnet torque motor illustrated in Fig. 4.1 is commonly used in the electrohydraulic servo valve. The torque motor consists of a armature mounted on flexure tube and suspended in the air gap of the magnetic filed. When current is passed through the coil, the armature ends become polarised and each end is attracted to one pole piece and repelled by the other. There are four air gaps. Two of them carry the sum of the permanent magnet and coil flux while other two carry the difference. Since the magnetic attractive force developed in the air gap is proportional to the square of the flux, the magnetic attractive force at the two diagonally opposite air gaps where both fluxes are added is larger than at the other two air gaps where both fluxes are canceled. Therefore, torque is developed on the torque motor armature which is proportional to the input differential current.

4.2 Torque Motor analysis

4.2.1 Fundamental voltage equation

When the quiescent current flows in each armature coil there is no net torque developed in the armature because the currents opposes each other. When the differential current exist, only then the torque get developed

The fundamental voltage equation of the torque motor is given by·

$$2\mu e_g = \left(R_c + r_p\right)\Delta i + 2N_c\frac{d\phi}{dt} \qquad (4\text{-}1)$$

Where R_c : Resistance of each coil (ohms)

r_p : Internal resistance of amplifier (ohms)

N_c Number of turns in each coil

ϕ_a Total magnetic flux through armature (Weber)

Δi Differential current

μ Amplifier gain for each side of the coil

e_g Signal voltage input to the amplifier

4.2.2 Magnetic flux circuit analysis

An approximate but adequate magnetic flux circuit analysis can be made by assuming that the four air gaps constitute the dominant reluctance in the circuit, that is, the reluctance of the magnetic materials are negligible in comparison with the reluctance of gaps Because of symmetry we can assume that the reluctances of diagonally opposite air gaps are equal and given by.

$$R_1 = \frac{g - x}{\mu_0 A_g} \tag{4-2}$$

$$R_2 = \frac{g + x}{\mu_0 A_g} \tag{4-3}$$

Where

R_1 Reluctances of gaps 1 and 3, (amp-turn/weber)

R_2 : Reluctances of gaps 2 and 4, (amp-turn/weber)

g : Length of air gap at neutral, (m)

x : Movement of armature tip from the neutral

A_g : Pole face area (m^2)

μ_0 : Permeability of the free space = $4 \pi 10^{-7}$ Henry / meter

With these assumption, the magnetic circuit can be represented by Fig 4 2. Since the circuit are symmetrical bridge, the flux through diagonally opposite air gaps are equal. The magnetic flux at each air gap can be given by

$$\phi_1 = \frac{\phi_g + \phi_c}{1 - \frac{x}{g}} \tag{4-4}$$

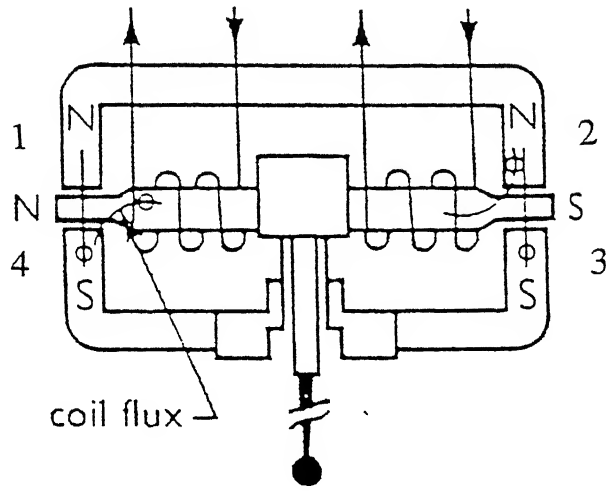

Fig. 4.1 Torque motor schematic view

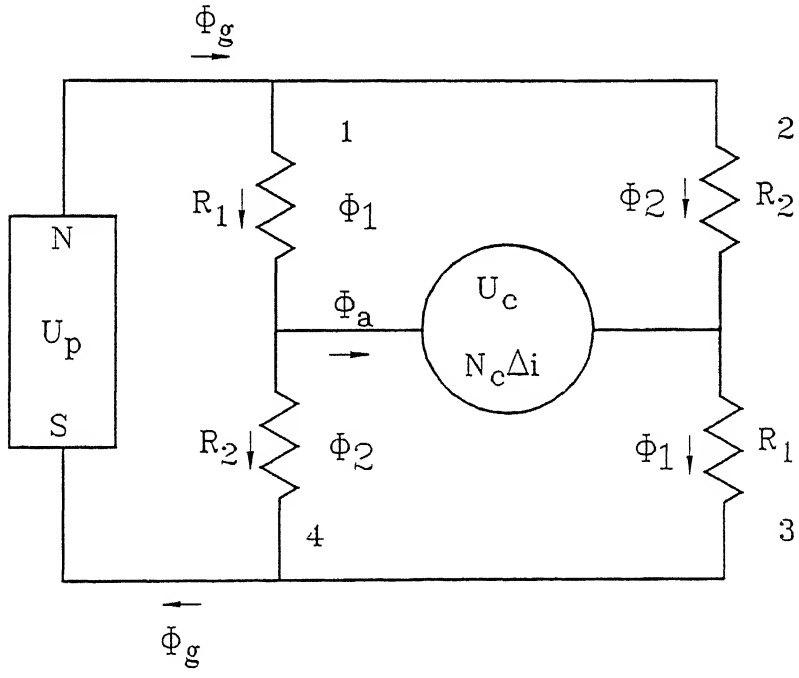

Fig. 4.2 Magnetic circuit of torque motor

$$\phi_2 = \frac{\phi_g - \phi_c}{1 + \frac{x}{g}} \tag{4-5}$$

Where ϕ_g Flux at each air gap at neutral

ϕ_c Flux due to control currents

$$\phi_g = \frac{U_p}{\frac{2g}{A_g \mu_0}} \tag{4-6}$$

$$\phi_c = \frac{U_c}{\frac{2g}{A_g \mu_0}} = \frac{N_c \Delta I}{\frac{2g}{A_g \mu_0}} \tag{4-7}$$

4.2.3 Torque Development

The magnetic force developed in the air gap is proportional to the square of the flux. The magnetic force developed in the air gap is given by

$$F = \frac{\phi^2}{2\mu_0 A_g} \tag{4-8}$$

The magnetic attractive force in the two air gaps at each end of armature are in opposite direction, the torque developed on the armature is given by

$$T_d = \frac{(\phi_1^2 - \phi_2^2)a}{\mu_0 A_g} \tag{4-9}$$

Substituting the values of ϕ_1 and ϕ_2 from the Eq (4-4) and Eq.(4-5) and after simplification we get the equation for the torque developed in the armature.

The torque developed is given by

$$T_d = \frac{\left(1-\frac{x^2}{g^2}\right)K_t + \left(1+\frac{\phi_c^{\,2}}{\phi_g^{\,2}}\right)K_m\theta}{\left(1-\frac{x^2}{g^2}\right)^2} \qquad (4\text{-}10)$$

Where

T_d : Total torque developed in the armature due to electrical current input (N.m)

x : Displacement of armature tip from the neutral position (m)

g : Length of each air gap at neutral (m)

ϕ_c : Flux due to control current (Weber)

ϕ_g : Flux in each of four air gaps when armature is at neutral (Weber)

Δi : Differential current in the coil (amp)

θ : Rotation of the armature (radian)

$$K_t = 2\left(\frac{a}{g}\right)^2 N_c\phi_g \qquad (4\text{-}11)$$

and

$$K_m = 4\left(\frac{a}{g}\right)^2 R_g\phi_g^{\,2} \qquad (4\text{-}12)$$

where

K_t : Torque constant of the torque motor for each coil (N-m/amp)

K_m : Magnetic spring constant of torque motor (N-m/rad)

R_g : Reluctance of each air gap (amp-turn/Weber)

$$R_g = \frac{g}{\mu_0 A_g} \qquad (4\text{-}13)$$

where μ_0 : permeability of the free space

A_g pole piece area

The detailed derivation Eq.(4-10) is mentioned in Ref. [1] and [4]

Torque motors are designed so that $(x/g)^2 << 1$ and $(\phi_g / \phi_c)^2 << 1$ to improve linearity and static stability and prevent knock down of the permanent magnets. So, neglecting these quantities, Eq (4-1) becomes

$$T_d = K_t \Delta i + K_m \theta \tag{4-14}$$

Applying Newton 's second law to the armature we can write

$$T_d = J_a \frac{d^2\theta}{dt^2} + B_a \frac{d\theta}{dt} + K_a\theta + T_l \tag{4-15}$$

Where

J_a · Inertia of the armature

B_a · Viscous damping coefficient of the armature

K_a Torsion spring constant of armature pivot

T_l Load torque on the armature

Combining Eq (4-14) and Eq.(4-15) and Laplace transforming yield

$$K_t \Delta I = J_a s^2\theta + B_a s\theta + (K_a - K_m)\theta + T_l \tag{4-16}$$

The load torque T_l consist of torque due to flow force of the nozzle jet and torque due to force feedback spring.

4.3 Flexure Tube Design

The flexure tube is made of Berrylium copper alloy. It is tubular in construction. Torque motor armature along with flapper and feedback wire rests on the flexure tube. This tube prevents the hydraulic fluid from entering the torque motor. The torque generated by the torque motor is transferred to the flexure tube as a pure bending load. The stiffness of the flexure tube is given as:

Stiffness = E I / (L_t) N-m/rad

where E Young's Modulus of the material

I Second moment of the area of cross-section and

L_t Length of the tube

$$I = \frac{\pi}{64}\left(d_0^{\,4} - d_i^{\,4}\right)$$

d_0 : Outer radius of the tube

d_i : Inner radius of the tube and

$d_0 = d_i + 2t$

where t is thickness of the tube

The Fig. 4.3 shows the plot of stiffness v/s thickness for different inner diameter of the tube of a fixed length (20 mm). Similar plot can be made for different lengths of the tube as per requirements.

4.4 Static Performance Characteristics

The developed torque Eq. (4-10) can be written in normalised form as

$$\frac{T_d}{\left(\frac{g}{a}\right)K_m} = \frac{(\alpha+\beta)(1+\alpha\beta)}{\left(1-\beta^2\right)^2} \tag{4-17}$$

where

$$\alpha \equiv \frac{\phi_c}{\phi_g} = \frac{N_c}{2\phi_g R_g}\Delta i \tag{4-18}$$

$$\beta \equiv \frac{x}{g} = \frac{a}{g}\theta \tag{4-19}$$

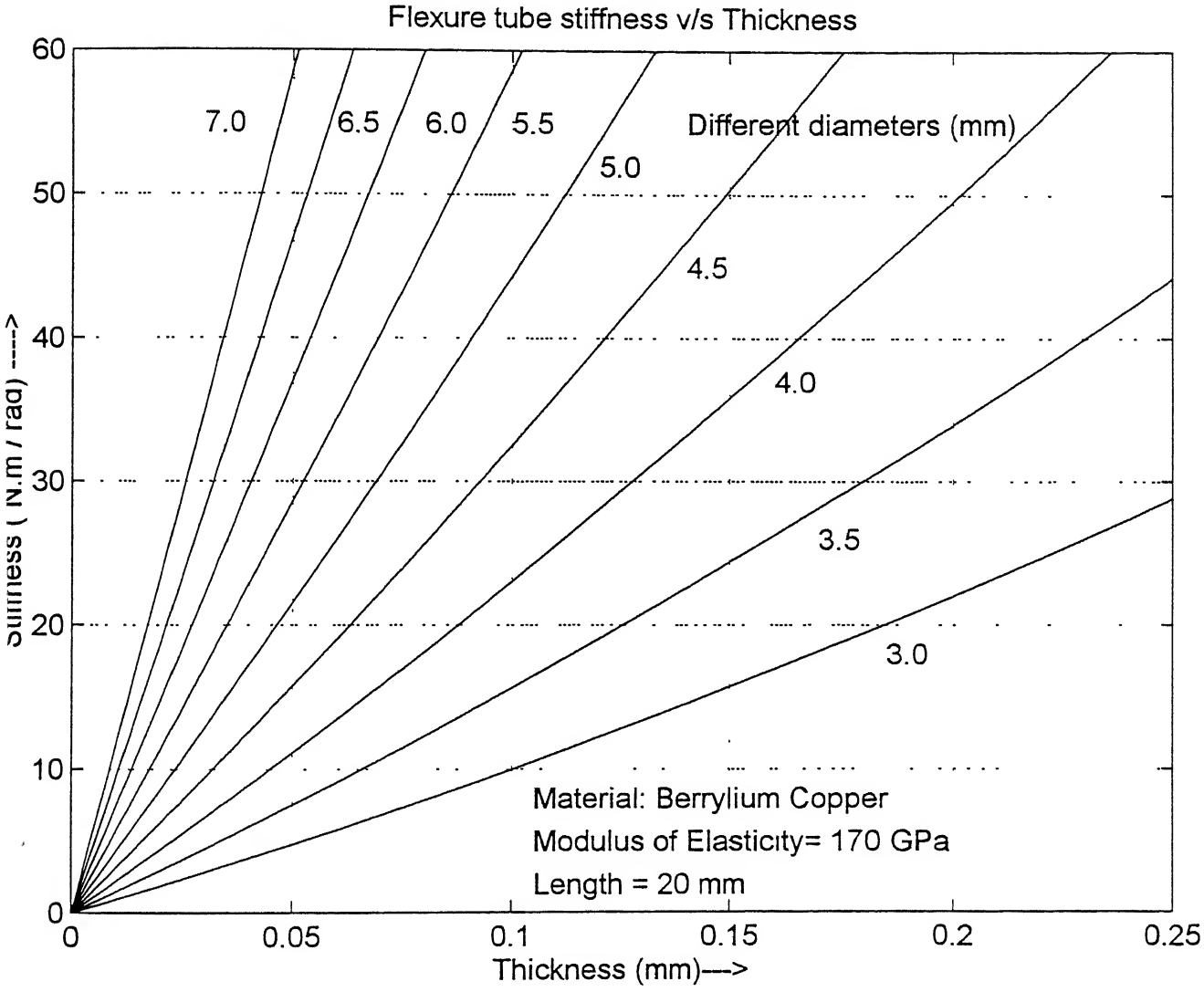

Fig. 4.3 Flexure tube stiffness characteristics

The Eq (4-17) can be plotted as shown in Fig 4-4

For static operation $T_d = K_a \theta + T_l$ which when combined with Eq (4-17), we get

$$\frac{K_m}{K_a}(\alpha+\beta)(1+\alpha\beta) = (1-\beta^2)^2\beta + \frac{(1-\beta^2)^2}{\left(\frac{g}{a}\right)K_a}T_l \qquad (4\text{-}20)$$

This equation describes the static characteristic curve of the torque motor with load In no load case when $T_l = 0$ and solving for α we get

$$\alpha = \frac{1+\beta^2}{2\beta}\left(\left\{1+\frac{K_a}{K_m}\left[\frac{2\beta(1-\beta^2)}{1+\beta^2}\right]^2 - \left(\frac{2\beta}{1+\beta^2}\right)^2\right\}^{1/2} - 1\right) \qquad (4\text{-}21)$$

Eq.(4-21) is plotted in Fig 4.5 and Fig 4.6 for various K_m / K_a ratios. From these figures it is clear that armature becomes unstable for $|x/g| > 1/3$ regardless of the value for (K_m / K_a)

It is also apparent that the slope or gain of the curve increases with the ratio K_m / K_a. The (ϕ_c / ϕ_g) ratio is kept below unity to avoid knockdown of the permanent magnet and linearity is controlled by the ratio of K_m / K_a

4.5 Dynamic performance Characteristics

The torque motor and servovalves are usually specified with the differential current as input. The transfer function from current input to flapper rotation can be obtained from Eq. (4-16) as

$$\frac{\theta}{\Delta I} = \frac{\dfrac{K_t}{K_a\left(1-\dfrac{K_m}{K_a}\right)}}{\dfrac{s^2}{\omega_m^2\left(1-\dfrac{K_m}{K_a}\right)} + \dfrac{B_a}{K_a\left(1-\dfrac{K_m}{K_a}\right)}s + 1} \qquad (4\text{-}22)$$

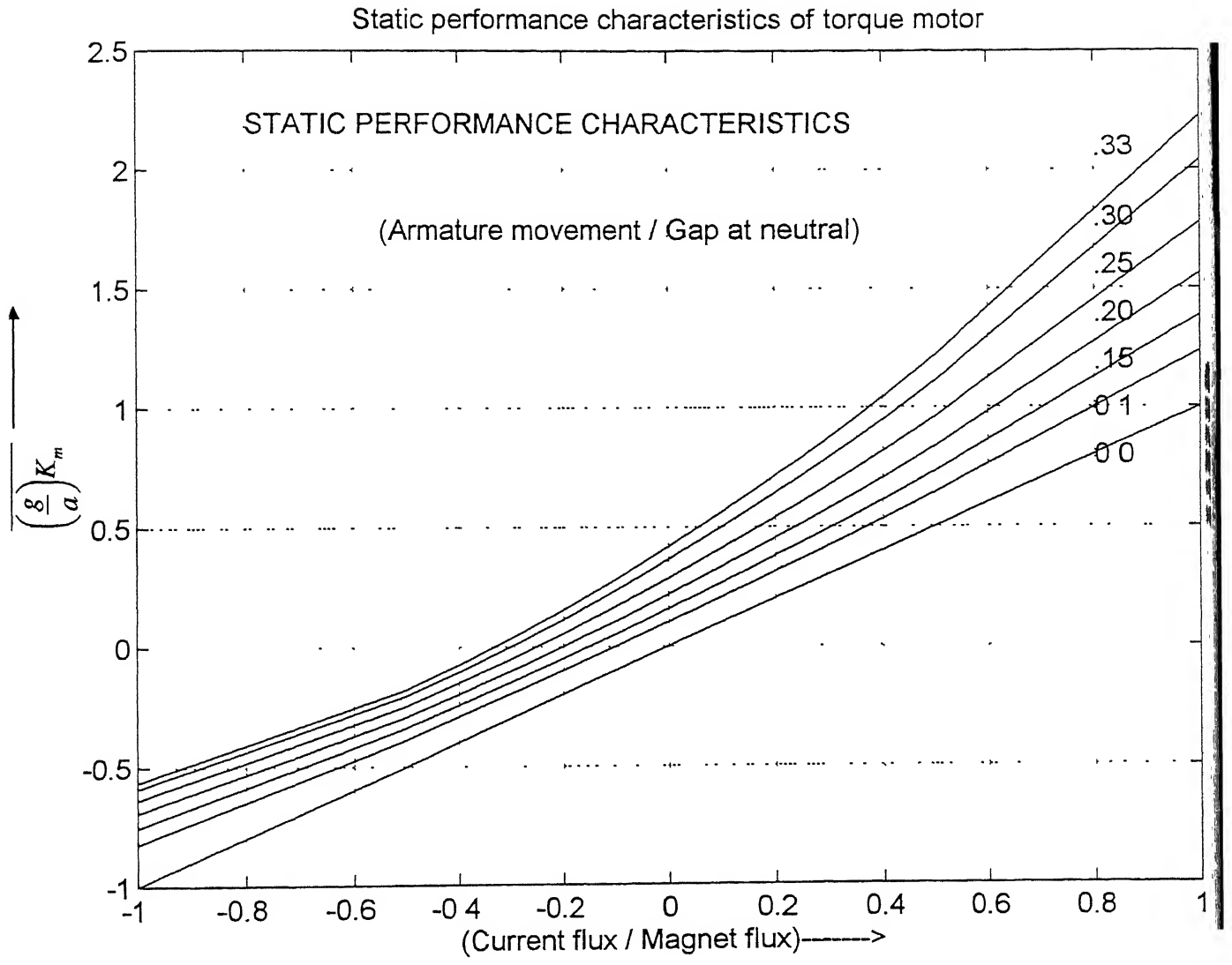

Fig. 4.4 Normalised plot of no load deflection v/s Flux ratio

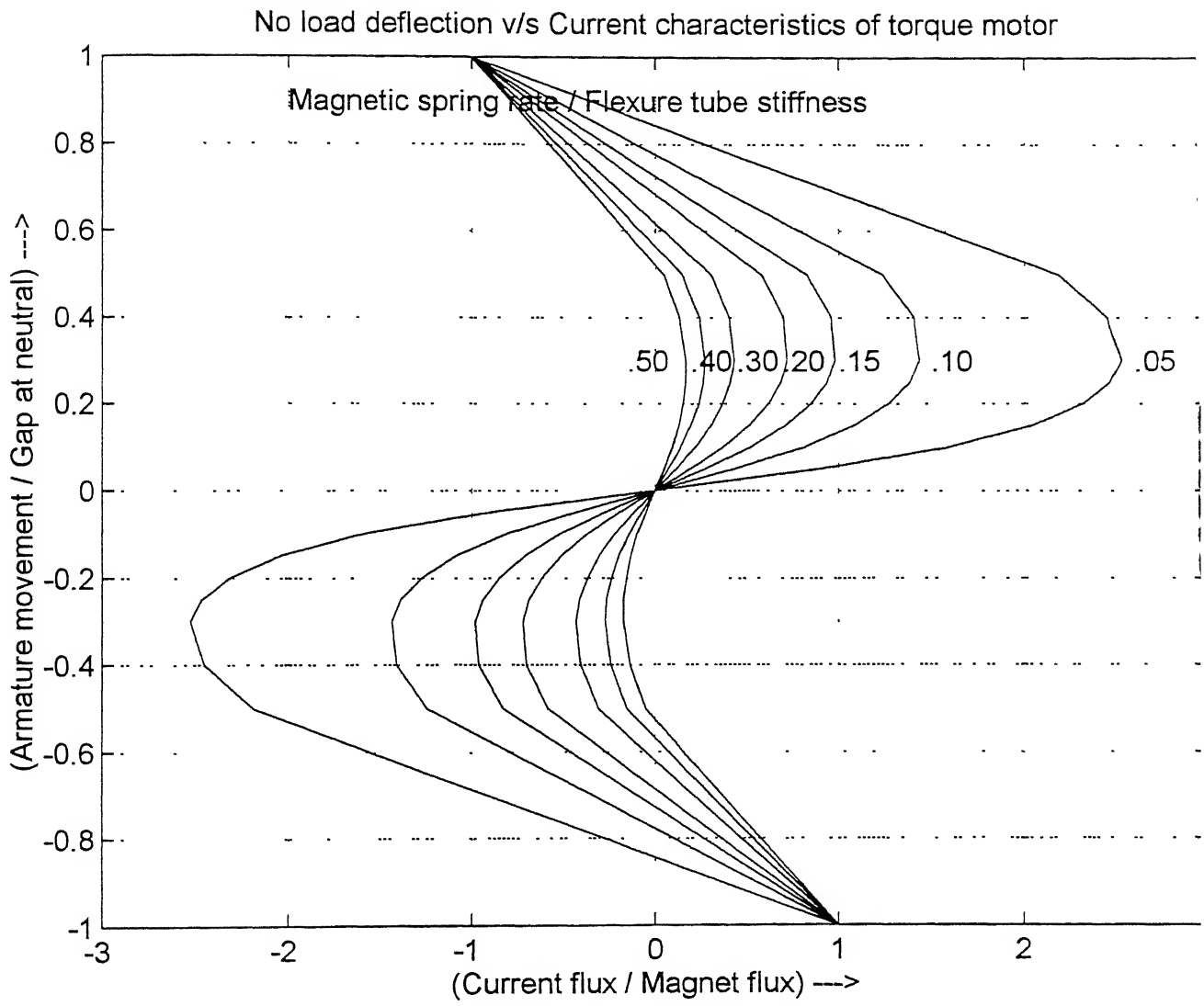

Fig. 4.5 Static performance characteristics of torque motor

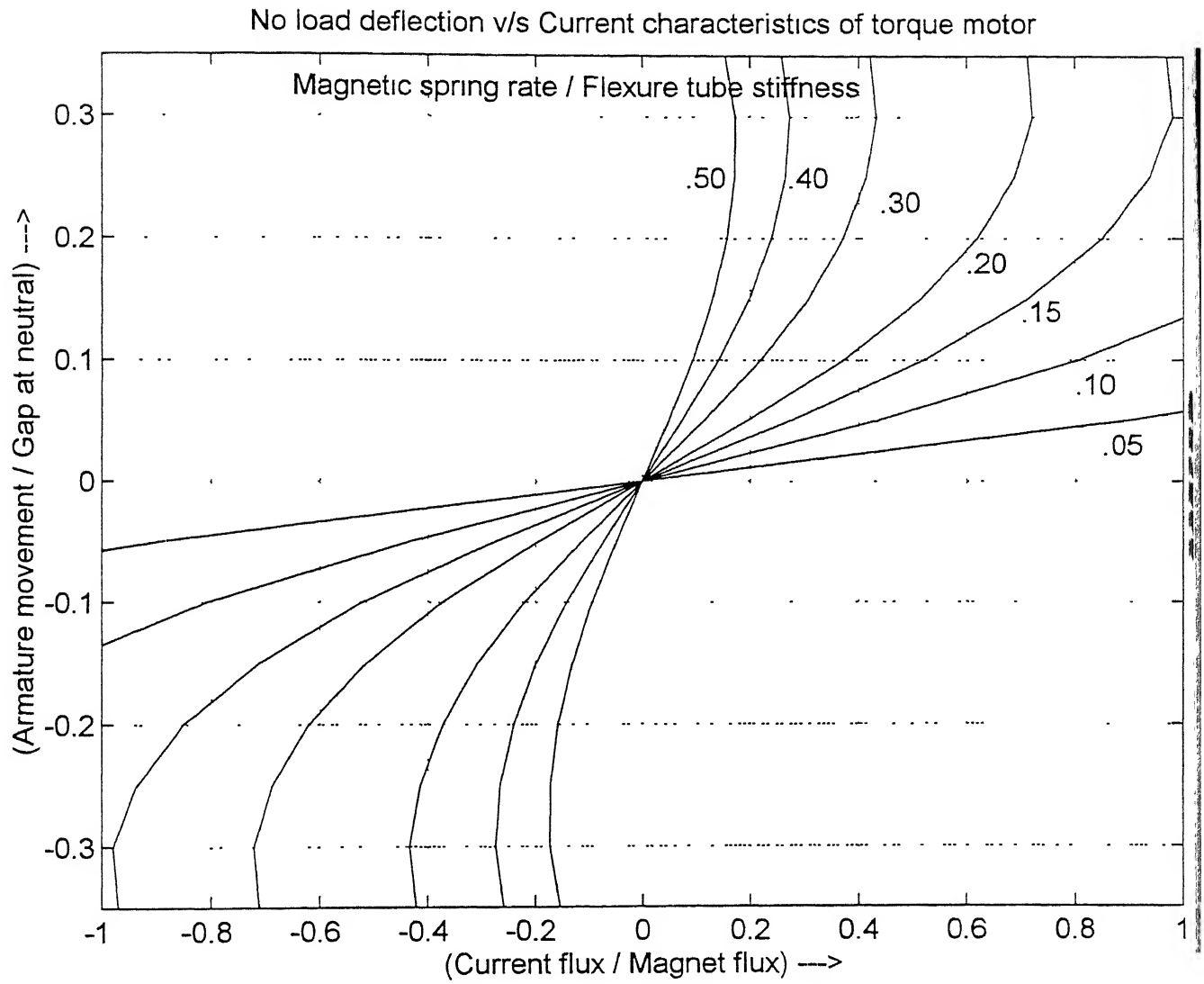

Fig. 4.6 Static performance characteristics of torque motor

where ω_m . Natural frequency of the torque motor armature

The frequency response plot of the Eq (4-22) is shown in the Fig. 4.7.

4.6 Summary

From static performance plot as shown in the Fig 4 4, we see that the total torque developed increases with the control current for all values of the armature rotation Similarly the developed torque also increases with the armature rotation for a constant value of current The non-linearity increases with control current as well as armature rotation.

In the frequency response plot of the torque motor has been obtained using very low damping ratio because it depends on the structural damping in the flexure tube. The gain is stable upto 100 Hz and natural frequency is quite high and has positive phase and gain margin.

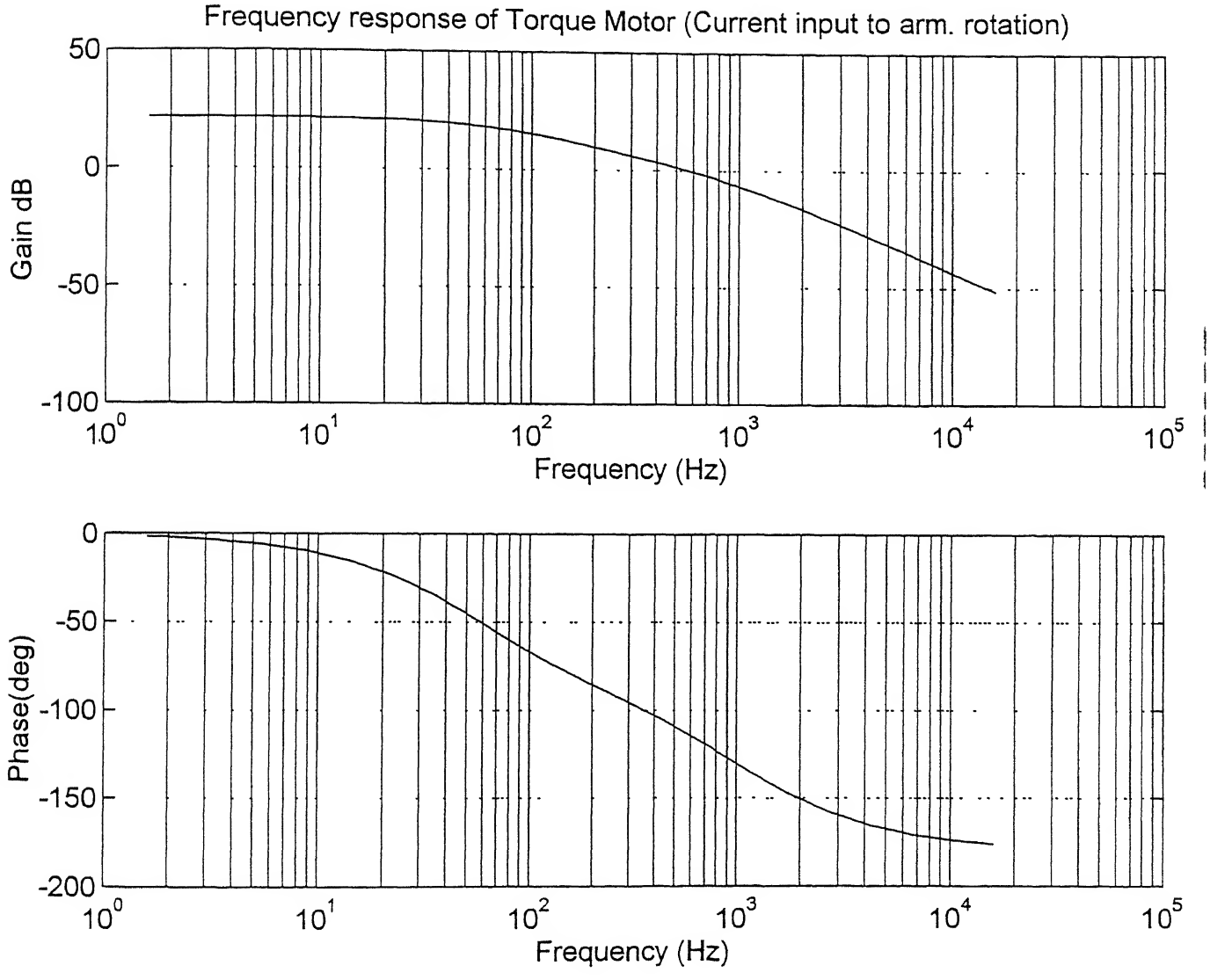

Fig. 4.7 Frequency response plot of torque motor

Chapter 5

5.1 Dynamic Analysis of Servovalve

Using the results obtained in Chapter 2 to Chapter 4 we can perform dynamic analysis of the force feedback servovalve The torque motor Eq.(4-16) and (3-17) can be combined into following equation

$$K_t \Delta I = J_a s^2\theta + B_a s\theta + K_{an}\theta + rP_{vl}a_n + (r+b)K_f[(r+b)\theta + \Delta x] \qquad (5\text{-}1)$$

where

r Distance between armature pivot and center of nozzle

b Distance between center of the nozzle and connecting point of the feedback spring to spool.

K_f Spring constant of the feedback spring, and

$$K_{an} = K_a - K_m - r^2\left(8\pi C^2_{df} x_{f0} P_s\right) \qquad (5\text{-}2)$$

In Eq (5-1), the flapper deflection $x_f = r\,\theta$ and total deflection of the feedback spring at its connecting point to the spool given as [(r+b)θ+ x)] has been used. In the Eq (5-1) $r\,P_{vl}\,a_n$ term is flow force moment which is negligibly small.

The response of the nozzle flapper valve controlling the spool when Laplace Transformed can be given as

$$A_s \Delta P_{vl} = M_s s^2 \Delta x + B_s s\Delta x + K_f\{(r+b)\theta + \Delta x\} + K_s \Delta x \qquad (5\text{-}3)$$

and

$$\Delta Q_{vl} = A_v s \Delta x \qquad (5\text{-}4)$$

where M_s · Mass of the spool

B_s Damping coefficient of spool including that due to transient flow force

A_s End area of the spool

Combining Eq (5-3) and (5-4) with nozzle flapper flow equation as given below

$$\Delta Q_{vl} = K_{q0}\Delta x_f - K_{c0}\Delta P_{vl}$$

we get

$$A_s s\Delta x + \frac{K_{c0}}{A_s}\left[M_s s^2\Delta x + B_s s\Delta x + K_f\{(r+b)\theta + \Delta x\} + K_s\Delta x\right] = K_{q0}\Delta x_f \qquad (5\text{-}5)$$

Neglecting the flow force term in Eq.(5-1) and combining with the Eq.(5-5) and keeping in mind that the value of K_{q0} is far greater that K_{c0} and hence neglecting K_{c0}, the Eq.(5-5) reduces to

$$\frac{\Delta x}{\Delta x_f} = \frac{K_{q0}}{A_s s} \qquad (5\text{-}6)$$

Thus the simplified block diagram is as shown in the Fig. 5-1. The gain constant of the loop transfer function for this block diagram is given by

$$K_v = \frac{r(r+b)K_f K_{q0}}{A_n[K_{an} + K_f(r+b)^2}} \qquad (5\text{-}7)$$

In order to keep K_v as large as possible, K_{an} should be as small as possible. Actual flow control servovalves are designed so that K_{an} is small.

The block diagram shown in Fig 5-1 has been analysed using the MATLAB software The frequency response is shown in shown in Fig. 5-2 and transient response is shown in the Fig. 5-3.

5.2 Summary

From the Fig. 5 2, it can be concluded that the gain of the system is constant upto 200 Hz. However the phase lag increases continuously. From the transient response, we can conclude that the system is quite stable and has high damping ratio. The system stabilises in approximately $5x10^{-3}$ second to the steady state value of 0.051. Also it can be concluded from the figure that the system time constant is of the order of 0 001 second.

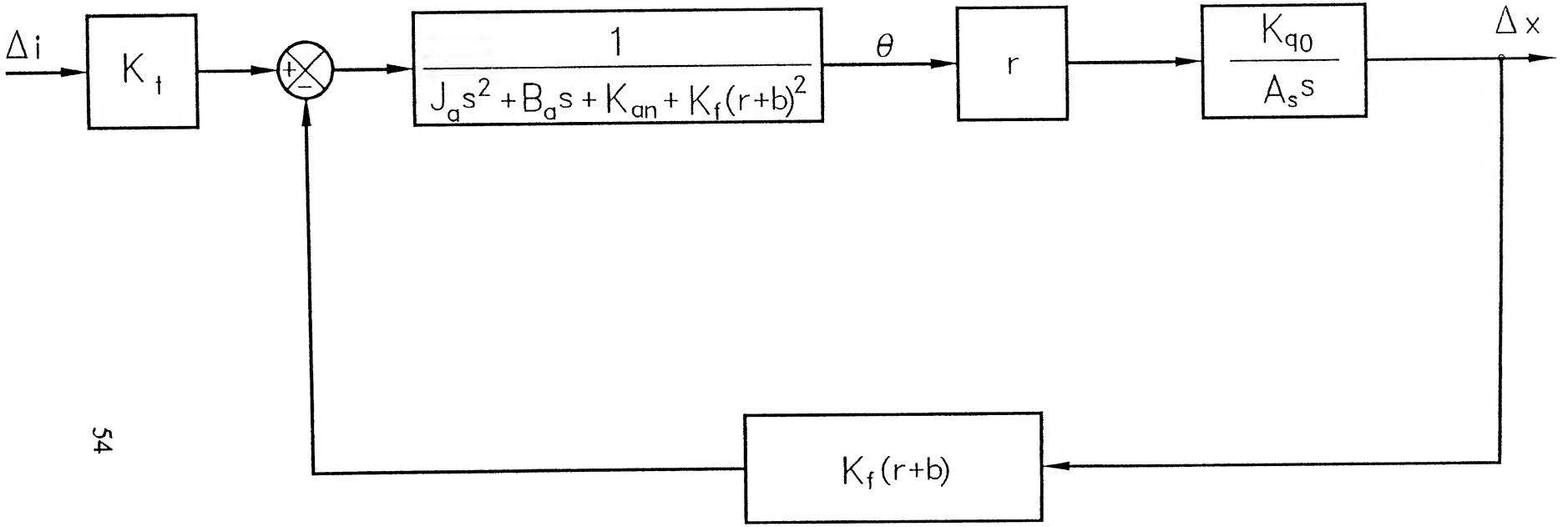

Fig. 5.1 Simplified Block Diagram of Servovalve

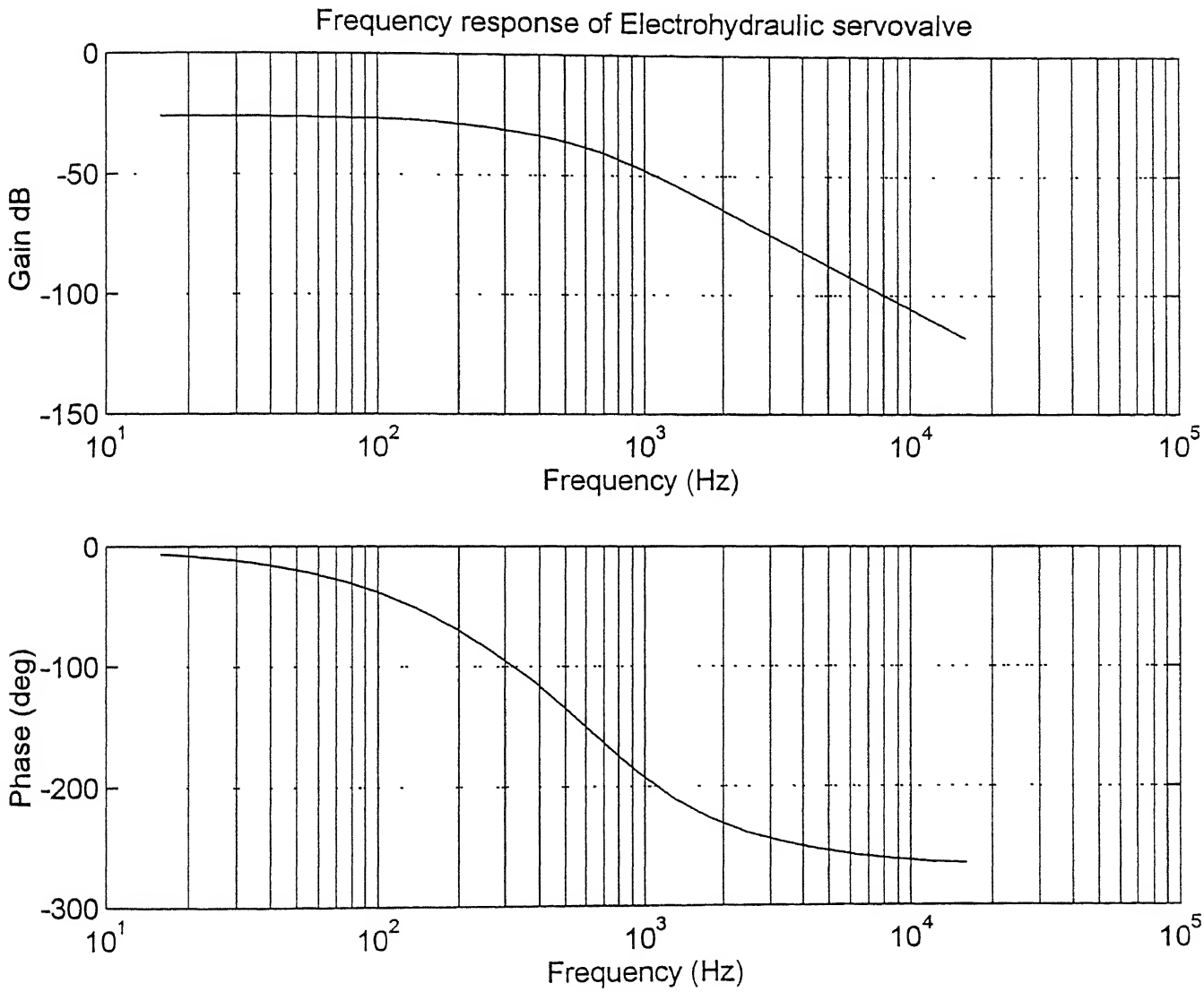

Fig 5.2 Frequency response of servovalve

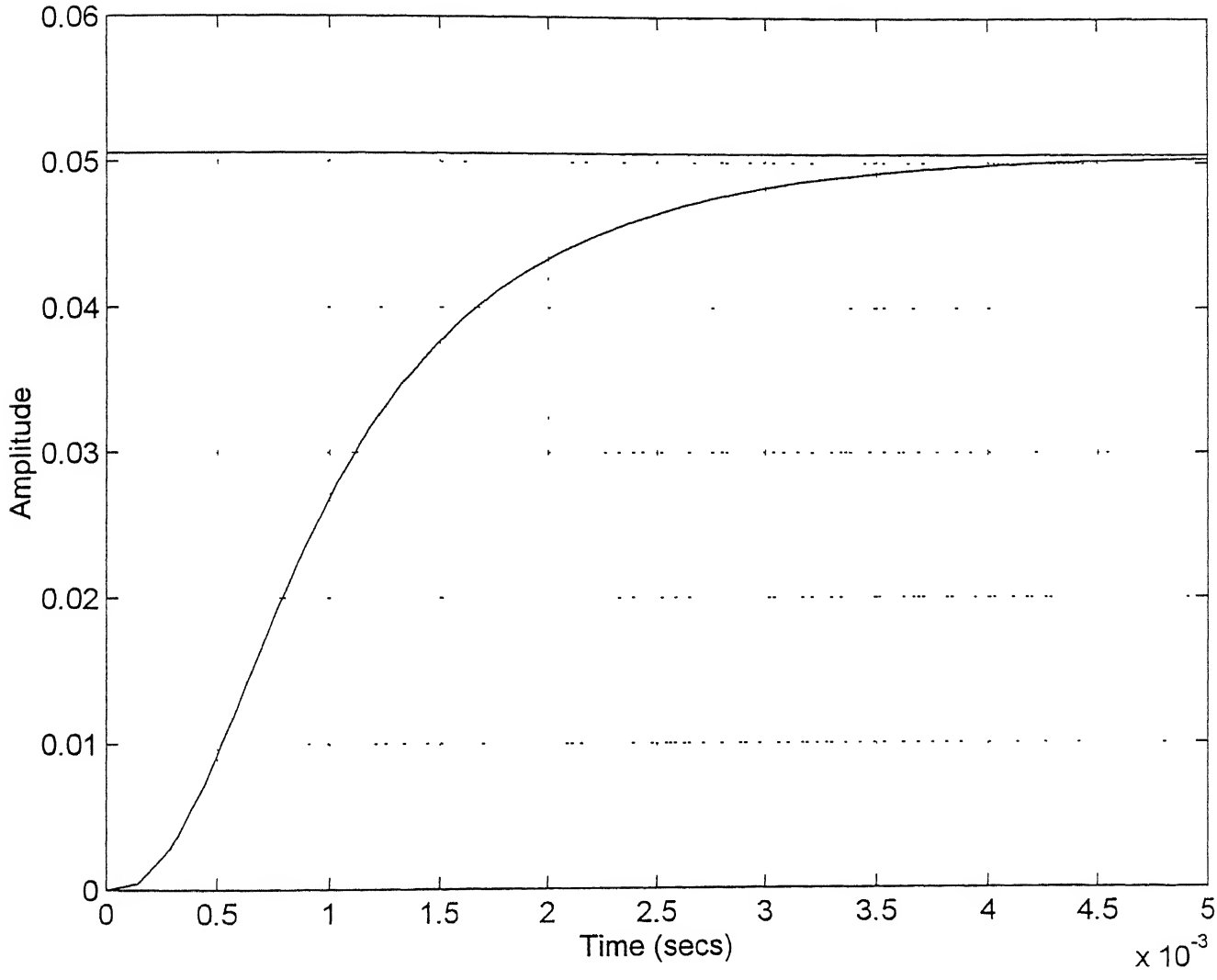

Fig. 5.3 Transient response of servovalve

CHAPTER 6

Design Methodology

6.1 Design of the spool valve

Spool valve dimensions are sized to satisfy load and pressure requirements There are several dimensions that must be maintained in the manufacture of the spool valve. They are as follows

- The width of porting lands must match the corresponding width in the sleeve.
- The distances between lands must match the corresponding dimensions in the sleeve
- Close tolerances must be maintained on the radial dimensions and on the squareness of the land edges

The above dimensions must be within the tolerances of few microns These tolerances are very important because they have pronounced effect on the flow gain and pressure sensitivity near null.

Three way as well as four-way valves are being used Three way valve have half the pressure sensitivity and resonance frequency of the four-way valve. The particular application dictates the choice However four-way valve are used in the majority of the cases, hence this has been selected for this work

Another important factor to be considered is that of number of lands to be placed on the spool. Two- land valve is shorter in length and simpler in construction But it has two disadvantages Firstly, it is not statically balanced and secondly the lands may get lodged if the ports consume a major portion of the periphery of the spool. These drawbacks are corrected in four land spool to provide sealing and centering functions[1]. However the spool becomes longer. The three-way land is also statically balanced and most widely used. So three-land four way spool has been considered in this work.

The shape of the ports depend on system requirements. Round ports are simple but have quite non-linear characters. With round ports flow gain is very low near null and increases from the null position and all servo performance parameters (error, bandwidth, stiffness, etc.) becomes worse with lower gain. In most high performance systems performance parameters can not be sacrificed like this and use of rectangular ports to obtain a linear flow gain is essential Therefore linear ports are optimum from the view point of good servo performance over abroad operation range. For a linear flow gain, the critical center valve is usual choice. However open center valves are useful in applications where the valve must be at the null position in high temperature environment for extended period of time and a continuous flow is required to maintain reasonable fluid temperature. Open center valves are required in constant flow systems Open center valves have two major disadvantages - increased flow gain near null and power loss

A critical center four-way spool valve with rectangular ports is by far the most common servo valve. Such a valve is characterised by area gradient w and maximum stroke x_{vm} and rated by load flow at maximum stroke with specified valve pressure drop.

6.1.1 Area Gradient

The valve area gradient is the principal parameter in the null flow gain and has direct influence on system stability. The flow gain must be compatible with gains of other in the system to yield the loop gain. The null flow gain must be determined and then the area gradient can also be computed from the null flow gain equation.

The area gradient w can be found using the Eq.(2-3) as

$$w = \frac{ql}{C_d x_{xm}\sqrt{\frac{P_v}{\rho}}} \qquad (6\text{-}1)$$

The maximum valve stroke can also be used to vary valve size. In general, the longer the stroke the better The longer stroke gives better resolution near null and improved performance with dirty fluids because dirt particles are flushed out and reduces the silting problem.

The design relation from flow saturation and valve strength point of view following point are important

- The spool rod diameter should be at least half of the spool diameter.

- The spool passage areas should be at least four times the maximum orifice area to prevent flow saturation

Once the area gradient w is selected, the minimum value of spool diameter is determined because ports may be at most full periphery of the spool Two or four rectangular ports symmetrically placed in the spool sleeve periphery is the most commonly used method of obtaining very low area gradient. The area gradient is then the total width of all slots at a particular orifice.

6.1.2 Spool Dimensions

Let approximate dimensions of the spool be as follows:

Spool rod diameter	= 0 5 x spool diameter
Length of spool	= 4 to 6 x spool diameter
Width of the spool	= 0.5 x spool diameter
Distance between spool lands	= 2 25 x width of the spool
Distance between middle spool	= 0.1x distance between spool lands

On the basis of approximate spool dimensions, mass of the spool is calculated. The contained volume of the fluid in the spool end chamber is calculated. The total volume of the fluid is estimated and total mass of the fluid as well as spool is calculated.

6.1.3 Hydraulic natural Frequency

The hydraulic natural frequency of the first stage is calculated as follows·

$$\omega_{hp} = \sqrt{\frac{2\beta_e A_s^2}{V_{op} M_t}} \qquad (6\text{-}2)$$

where A_s Spool end area

M_t Mass of the spool and hydraulic fluid which is getting accelerated

V_{op} Volume of hydraulic fluid at the end of the spool

β_e Effective bulk modulus of the hydraulic fluid

10 % of the ω_{hp} gives the crossover frequency for sufficient stability margin. Velocity coefficient (open loop gain) is taken to be equal to 10% of the hydraulic natural frequency. The first stage flow gain is obtained from

$K_{qp} = K_{vp} \cdot A_s$

Where A_s Spool end area

K_{qp} · Nozzle flapper flow gain

Once nozzle-flapper flow gain (K_{qp}) is obtained, the remaining nozzle-flapper design parameters are determined as shown below in the following section

6.2 Design of Flapper Valve

6.2.1 Nozzle diameter

The design of flapper starts from the determination of the flow gain from the system requirements Once the null flow gain is established, the nozzle diameter is found from (3-9) as follows·

$$d_n = \frac{K_{q0}}{\pi C_{df}\sqrt{P_s/\rho}} \tag{6-3}$$

6.2.2 Null Flapper Clearance

The null flapper clearance x_{f0} should be as small as possible to achieve largest pressure sensitivity and smallest null leakage. It must be large enough to permit passage of the dirt particles expected in the fluid. A maximum value of the null clearance is established by requiring the curtain area to be less than one fourth the nozzle area. This ensures that the curtain area is the controlling orifice Therefore,

$$\pi d_d\, x_{f0} \le \left(\frac{1}{4}\right)\frac{\pi d_n^{\,2}}{4} \tag{6-3}$$

which on simplification gives

$$x_{f0} \le \frac{d_n}{16} \tag{6-5}$$

Thus the maximum value of null clearance is $d_n/16$. Once d_n and x_{f0} is known, the upstream orifice diameter d_0 is determined form (3-2).Therefore,

$$d_0 = 2\left(\frac{C_{df}}{C_{d0}} d_n x_{f0}\right)^{1/2} \tag{6-6}$$

Note: 1. Some researchers have reported the experimental negative spring rate to be equal to the three times the theoretical value. So is better to use the experimental value if available as far as possible.

2. The upstream orifice is 'short tube' type Consequently C_{d0} will be in the range 0.8 to 0.9.

3. In this report the ratio of the discharge coefficient C_{df}/C_{do} equal to 0.8 has been used.

6.2.3 Feedback spring design

The feedback spring is very important as far as feedback is concerned. It is this spring which senses the driving force acting on the spool to stroke When the driving force acts, the feedback spring bends and stays at a position where the moment due to the spool driving force in conjunction with spool flow force balances the driving torque of the torque motor The feedback spring can be either leaf spring type or simple or linearly varying cross-section wire When the spring cross-section (circular or rectangular) is uniform through out its length, the spring rate is given as

$$K_f = \frac{3EI}{L^3} \text{ N/m} \tag{6-7}$$

Where E . Young's Modulus of the material of the spring

I Second moment of area about bending plane

L · Length of the spring

In case the spring wire is linearly varying cross-section, the stiffness can be obtained by finding the deflection equation by energy method. The final equation for the stiffness can be given as

$$K_f = \frac{K^3 E\pi}{64Z} \text{N/m} \tag{6-8}$$

where $K = \frac{d_2 - d_1}{L}$

and

$$Z = \left[\left(-\frac{1}{d_2} - \frac{d_1^2}{3d_2^3} + \frac{d_1}{d_2^2}\right) - \left(-\frac{1}{d_1} - \frac{d_1^2}{3d_1^3} + \frac{d_1}{d_1^2}\right)\right] \tag{6-9}$$

d_2 : Maximum diameter of the wire

d_1 . Minimum diameter of the wire

6.2.4 Armature Spring Rate

The armature spring rate is sized in accordance with following relation:

$$K_{vf} = \left(\frac{r}{r+b}\right)\frac{K_{qp}}{A_s} \tag{6-10}$$

K_{vf} . Velocity constant spool positioning loop (Type 1 , rad/sec)

The feedback spring rate K_f should be large enough to satisfy the following equation to ensure stability.

$$\left(\frac{r}{r+b}\right)\left(\frac{A_n}{A_s}\right)\frac{0.43wP_s}{K_f} < 1 \tag{6-11}$$

and to keep torque motor natural frequency ω_{mf} high so that flapper natural frequency K_{vf} is not limited to low value. However K_f should be small to minimise the input current required for full stroke and to minimise torque motor size

Note: The Eq (6-11) has been referred as **Condition 1** in the following sections

The spool stroke should be large enough to improve resolution and silting problem and to reduce over-all servovalve size.

6.3 Torque motor parameters

As we have seen in chapter 4 that net spring rate of the torque motor is given by following relation.

$$K_{an} = K_a - K_m - r^2\left(8\pi C_{df}{}^2 P_s x_{f0}\right) \tag{6-12}$$

To maximise the gain constant, the servovalves are usually designed so that $K_{an} = 0$, that is,

$$K_a = K_m + r^2\left(8\pi C_{df}{}^2 P_s x_{f0}\right) \tag{6-13}$$

Thus mechanical spring rate on the torque motor armature just balances the negative spring rates due to magnetic s and to flow forces on the flapper. With this design criteria the velocity constant reduces to

$$K_{vf} = \left(\frac{r}{r+b}\right)\frac{K_{qp}}{A_s} \tag{6-14}$$

The feedback spring length b should be kept short to maximise the gain. The maximum value of K_{vf} is limited by stability considerations to less than about 20% of the lowest natural frequency in loop The loop containing torque motor dynamics has a cubic characteristic equation which has a quadratic factor at a around the natural frequency

$$\omega_{mf} = \left[\frac{K_f(r+b)^2}{j_a}\right]^{1/2} \tag{6-15}$$

The other natural frequency is ω_{hp} But ω_{mf} is lower one Hence the stability criteria for the force feedback loop becomes

$$K_{vf} < 0.2\omega_{mf} \tag{6-16}$$

K_{vf} is the lowest of the break frequencies in the dynamic response of the force feedback servovalve The lag at this frequency dominates servovalve response and is often used as an approximation of servovalve dynamics

Note: Eq. (6-16) has been referred as **Condition 2** in the following sections.

For steady state operation $x_f \approx 0$ and spool position is related to differential current by

$$x_v = \frac{K_t}{(r+b)K_f}\Delta i \tag{6-17}$$

which can be substituted in the valve port flow equation to obtain pressure- flow curves. As per the above equation K_t must be large as practical to improve the resolution and silting performance and to reduce over-all servovalve size

6.3.1 Armature Parameters

The armature length and the maximum armature movement at the center of the pole piece are assumed on the basis of the space limitation. The armature movement corresponds with the flapper movement since the angular rotation of the armature and flapper is same. The gap between armature and pole piece at neutral is taken at least three times more than the armature movement at the pole piece for the stability purpose.

The permanent magnet flux density can be taken to be the maximum possible value for minimising the magnet weight. Once the flux density is decided, other torque meter parameters are determined as below·

6.3.1.1 Reluctance of Air Gap

The reluctance of the air gap at neutral is calculated using Eq. (4-13) as

$$R_g = \frac{g}{\mu_0 A_g} \tag{6-18}$$

6.3.1.2 Magnetic Spring Constant

The magnetic spring constant is determined as

$$K_m = 4\left(\frac{a}{g}\right) R_g \phi_g^{\,2} \tag{6-19}$$

6.3.1.3 Number of Turns

The ratio of control current flux to permanent magnet flux is taken below unity to avoid knock down of the permanent magnet The rated current is decided on other considerations The number of turns in each coil is calculated as

$$N_c = \frac{\alpha 2 \phi_g R_g}{\Delta i} \tag{6-20}$$

Variables are as discussed in Chapter 4.

6.3.1.4 Torque Constant

The torque constant is determined using Eq (4-11)

6.3.1.5 Torque Development

The developed torque is calculated as per Eq (4-14)

6.3.1.6 Self Inductance

The self inductance (L_c) of each coil is calculated as

$$L_c = \frac{N_c^2}{R_g} \tag{6-21}$$

6.1.3.7 Resistance of coil

Once the number of turns are known and coil diameter is decided, the length of the wire is determined and the resistance of the coil is determined:

$$R = \rho \frac{l}{a} \tag{6-22}$$

where ρ · Specific resistance of the wire material

l : Length of the wire

a · Cross-sectional area of wire of the coil

6.3.1.8 Impedance of the coil

The impedance of each coil is determined as ·

$$\text{Im}\,pedence = \sqrt{(\text{Re}\,sis\,\text{tan}\,ce)^2 + (2\pi nL_c)^2} \tag{6-23}$$

where n · Frequency of the signal current (say 100 Hz)

6.3.2 Flexure Tube

The angular stiffness of the flexure tube is selected 2.5 times or more of the magnetic spring constant of the torque motor The length and inner diameter of the tube is decided on space available basis and thickness can be obtained from Fig. (4-4).

RESULTS AND CONCLUSION

7.1 Conclusion

An analysis of various design aspects of electrohydraulic servovalve and its subsystem has been attempted using the cited references and literature. Based on the design methodology given in Chapters 2 to 6, the basic design parameters of the servovalve has been computed for a particular specified servovalve specification. These values have been taken up for the further design and analysis. An application program has been developed in MATLAB language. The sample output of the application has been included in Appendix A.

For linear behaviour of the servovalve flow, rectangular control port has been selected. The rectangular control ports dimensions have been calculated based on the fundamental equation of discharge through orifice. The spool diameter is based on full periphery slot in the sleeve. However full periphery slot are rarely used. So higher diameter spool can be selected and the port area gradient can be distributed in two or four intervals around the spool. The other dimensions of the spool has been calculated on the basis of the spool diameter. The spool null coefficients, driving force, flow force, spring rate, damping coefficient have been calculated. The design parameters have been checked to satisfy the stability criteria.

The flapper discharge coefficient of the variable orifice has been assumed as mentioned in the literature and accordingly other design parameters has been determined. In the hydraulic amplifier design, the nozzle diameter, fixed up stream orifice, the net force on the flapper due to flow impingement, feedback wire stiffness etc. have been calculated. Frequency response analysis of the armature flapper has been carried out. The frequency has been plotted.

7.2 Further Extension Required

Further work should be done in order to develop the design. The required flow gain, nozzle/flapper discharge coefficient, flow forces, damping coefficients and ratios of spool, flapper and torque motor should be measured experimentally and the design be modified accordingly. The elaborate experiments and tests should be carried out to validate the assumption made. In short, further work suggested are:

- Detailed engineering design of parts, assemblies and sub assemblies
- Extensive testing and experimentation and documentation.
- Design refinement of flexure tube, flapper, feedback wire and spool
- Elaborate torque motor design, analysis and fabrication and tests.

ERENCES

Meritt Herbert E, Hydraulic control systems, John Wiley and Sons , Inc. New York, 1967

Blackburn John F, et al , Fluid Power Control, John Wiley and Sons, New York 1960

Guillon M , Hydraulic Servo Systems, Analysis, & Design, Butterworth , London, 1969

Oshima Yasujiro , Electrohydraulic components page 241-280, Trends in Control Components , Edited by Nalecz Maciej, North Holland/ American Elsevier, Oxford / New York, 1974

Catalogues of Electrohydraulic Servovalve manufacturers,Moog Inc., 1965 and Dowty Boulton Paul Ltd , 1981

Technical Bulletin 103, Moog Inc., New York, 1965

MATLAB Users Guide and Reference Manual, The Math Works Inc , USA, 1995

APPENDIX A

ASSUMPTION: HYDRAULIC POWER SUPPLY USES VARIABLE DELIVERY PUMP

NOTE : FOR MAXIMUM POWER TRANSFER AND EFFICIENCY $P_l / Ps = 2/3$

SUPPLY PRESSURE = 20 7 MPa

LOAD PRESSURE = 13.8000 MPa

OPERATING EFFICIENCY OF SERVO VALVE CONTROLLED ACTUATOR = 66.6667 %

RATED FLOW = 26 lpm

MAXIMUM SPOOL MOVEMENT = 0 5 mm

VALVE AREA GRADIENT OBTAINED = 15.5825 mm

MAXIMUM VALVE PORT FLOW AREA =7 79124 mm^2

RATED FLOW AT 6 9 MPa VALVE PRESSURE DROP = 3 46667 x 10^{-6} m^3 /sec

SPOOL NULL CO-EFFICIENCY FOR CRITICAL CENTER VALVE

NULL FLOW GAIN OF SPOOL = 1.50 m^3 / sec / m

NULL PRESSURE COEFFICIENT OF SPOOL = 0.000000 m^3/ sec/ Pa

NULL PRESSURE SENSITIVITY OF SPOOL =3002.6 Mpa / mm

CENTRE FLOW WITH BLOCKED LOAD PORTS AND CENTERED SPOOL =10348.69 mm^3/ sec

DAMPING COEFFICIENT FOR SPOOL = 0.00359667

NULL COEFFICIENT FOR UNDERLAP SPOOL

NULL FLOW GAIN SPOOL = 3 00 m^3/ sec / m

NULL PRESSURE COEFFICIENT SPOOL (m^3/ sec / Pa)= 0.000145 m^3/ sec/ Pa

NULL PRESSURE SENSITIVITY SPOOL =20700 MPa / mm

CENTRE FLOW THROUGH VALVE (UNDERLAP) WITH BLOCKED LOAD PORTS & CENTERED SPOOL =6004.44 mm^3/ sec

SPOOL PRELIMINARY DIMENSIONS

MINIMUM SPOOL DIAMETER = 7.54252 mm

MINIMUM SPOOL ROD DIAMETER = 4.14838 mm

MINIMUM SPOOL END AREA = 44.681 mm^2

SPOOL DIAMETER SELECTED =7.54 mm

SPOOL ROD DIAMETER =4.147 mm

SPOOL END AREA =44.6511 mm^2

WIDTH OF SPOOL LAND = 3.77 mm

DISTANCE SPOOL LANDS = 8.4825 mm

TOTAL LENGTH OF SPOOL LENGTH (ls) = 45.24 mm

DISTANCE BETWEEN MID TWO SPOOL LANDS = 0.84825 mm

MASS OF SPOOL =11.4289 grams

HYDRAULIC NATURAL FREQUENCY = 19291.3 rad/sec

HYDRAULIC NATURAL FREQUENCY = 3070 3 Hz

SPOOL SPRING RATE = 46020 9 N/m

DESIGN OF FEEDBACK SPRING

(Linearly varying circular section)

LENGTH OF FEEDBACK SPRING WIRE =18.5400 mm

SELECTED FEEDBACK WIRE MAXIMUM DIAMETER = 1.415 mm

SELECTED FEEDBACK WIRE MINIMUM DIAMETER = 0.8 mm

SPRING CONSTANT OF SELECTED WIRE =9951.1866 N/m

VELOCITY COEFFICIENT = 906.364 rad/sec

VELOCITY COEFFICIENT = 144.252 Hz

FLAPPER VALVE ANALYSIS & DESIGN

CENTRAL FLOW = 2920 9253 mm^3/sec

DIAMETER OF NOZZLE = 0 27128 mm

NOZZLE-FLAPPER GAP = 0.016955 mm

DIAMETER OF FIXED INLET ORIFICE = 0.12132 mm

FLOW GAIN (FLAPPER) = 0.0861 m^3 / sec / m

PRESSURE SENSITIVITY COEFFICIENT (FLAPPER) =1220.88 MPa/mm

NULL FLOW PRESSURE COEFFICIENT = 0 0000

CHECK FOR STABILITY OF SERVOVALVE

SPOOL POSITION LOOP IS TYPE 1 SERVO VALVE

CONDITION 1 for stability is SATISFIED

NATURAL FREQUENCY OF FIRST STAGE = 5319.84 rad/sec

NATURAL FREQUENCY OF FIRST STAGE = 846.679 Hz

CONDITION 2 FOR STABILITY IS SATISFIED

CALCULATION OF RESISTANCE AND INDUCTANCE PER COIL

COIL CONNECTION SELECTED IS INDIVIDUAL COIL

RATED CURRENT (milli ampere) = 10

SELECTED RATIO OF ARMATURE MOVEMENT AND GAP AT NEUTRAL = 0.25

VALUE OF ARMATURE MOTION IN AIR GAP (mm) = 0.0148188

ARMATURE ROTATION = 0.00103195 rad

ARMATURE CENTER MOVEMENT = 0.0148188 mm

AIR GAP AT NEUTRAL = 0.0592753 mm

FLUX DENSITY SELECTED FOR PM (ALNICO VI) = 0.6 Weber / m^2

VALUE OF Ka - Km = 0.97531

THE RATIO OF Ka and Km SELECTED = 5

NO. OF TURNS PER COIL CALCULATED =3892

RATED CURRENT =10 ma

POLE PIECE AREA = 10.2 mm^2

SPECIFIC RESISTANCE OF WIRE =1 73x 10^{-8} Ω - m

LENGTH OF THE COIL SELECTED = 8 mm

DIAMETER OF THE COIL SELECTED = 5.6 mm

DIAMETER OF THE COIL WIRE SELECTED = 0.045 mm

REQUIRED RESISTANCE PER COIL = 882.46 Ω

REQUIRED INDUCTANCE PER COIL = 3.27553 Henry

IMPEDANCE OF EACH COIL =2239.29 Ω @ 100 Hz

ARMATURE RADIUS = 14 36 mm

TORQUE CONSTANT OF TORQUE MOTOR =11.5408 N-m/amp

MAGNETIC SPRING CONSTANT OF TORQUE MOTOR = 40.6619 N-m/rad

MECHANICAL TORSION SPRING CONSTANT OBTAINED = 41.6372 N-m/rad

MOMENT OF INERTIA OF FLAPPER = 4 3 x10^{-7} kg-m^2

TIME CONSTANT = 0.00110331 second

INERTIA OF ARMATURE AND ATTACHED LOAD (Kg . m^2) = 4.3x 10^{-7}

VISCOUS DAMPING COEFFICIENT ARMATURE MOUNTING (N-sec / m) = 0.003

NATURAL FREQUENCY OF TORQUE MOTOR ARMATURE =1683.81 rad / sec

NATURAL FREQUENCY OF TORQUE MOTOR ARMATURE =267 986 Hz

DAMPING RATIO TORQUE MOTOR = 0.1

RISE IN TEMP DUE TO OIL FLOW = 3 97763 °C

End